AIMS Mathematics, 8(3): 6136–6166.
DOI: 10.3934/math.2023310
Received: 17 October 2022
Revised: 12 December 2022
Accepted: 19 December 2022
Published: 30 December 2022

http://www.aimspress.com/journal/Math

Research article

Stability analysis of SARS-CoV-2/HTLV-I coinfection dynamics model

A. M. Elaiw[1,*], **A. S. Shflot**[1,2] **and A. D. Hobiny**[1]

[1] Department of Mathematics, Faculty of Science, King Abdulaziz University, P.O. Box 80203, Jeddah 21589, Saudi Arabia

[2] Department of Mathematics, Faculty of Science, King Khalid University, P.O. Box 960, Abha 61421, Saudi Arabia

* **Correspondence:** Email: aelaiwksu.edu.sa@kau.edu.sa.

Abstract: Although some patients with coronavirus disease 2019 (COVID-19) develop only mild symptoms, fatal complications have been observed among those with underlying diseases. Severe acute respiratory syndrome coronavirus 2 (SARS-CoV-2) is the causative of COVID-19. Human T-cell lymphotropic virus type-I (HTLV-I) infection can weaken the immune system even in asymptomatic carriers. The objective of the present study is to formulate a new mathematical model to describe the co-dynamics of SARS-CoV-2 and HTLV-I in a host. We first investigate the properties of the model's solutions, and then we calculate all equilibria and study their global stability. The global asymptotic stability is examined by constructing Lyapunov functions. The analytical findings are supported via numerical simulation. Comparison between the solutions of the SARS-CoV-2 mono-infection model and SARS-CoV-2/HTLV-I coinfection model is given. Our proposed model suggest that the presence of HTLV-I suppresses the immune response, enhances the SARS-CoV-2 infection and, consequently, may increase the risk of COVID-19. Our developed coinfection model can contribute to understanding the SARS-CoV-2 and HTLV-I co-dynamics and help to select suitable treatment strategies for COVID-19 patients who are infected with HTLV-I.

Keywords: COVID-19; SARS-CoV-2; HTLV-I; coinfection; global stability; Lyapunov function
Mathematics Subject Classification: 34D20, 34D23, 37N25, 92B05

1. Introduction

In November 2019, a dangerous type of virus named severe acute respiratory syndrome coronavirus 2 (SARS-CoV-2) appeared first in Wuhan, China. This virus infects the human body and causes coronavirus disease 2019 (COVID-19), which can lead to death. According to the update provided by the World Health Organization (WHO) on December 4, 2022 [1], over 641 million

confirmed cases and over 6.6 million deaths have been reported globally. SARS-CoV-2 is transmitted to people when they are exposed to respiratory fluids carrying infectious viral particles. The implementation of preventive measures such as hand washing, using face masks, physical and social distancing, disinfection of surfaces and getting the COVID-19 vaccine can reduce SARS-CoV-2 transmission. Ten vaccines for COVID-19 have been approved by the WHO for emergency use. These include Novavax, Bharat Biotech, Serum Institute of India (Novavax formulation), Sinopharm, Pfizer/BioNTech, Sinovac, Janssen (Johnson & Johnson), Oxford/AstraZeneca, Serum Institute of India (Oxford/AstraZeneca formulation) and that presented in [2].

SARS-CoV-2 is a single-stranded positive-sense RNA virus that infects epithelial cells. SARS-CoV-2 can lead to acute respiratory distress syndrome, which has high mortality rates, particularly in patients with other viral infections [3]. It was discovered in [4] that, 94.2% of individuals with COVID-19 were also coinfected with several other microorganisms, such as fungi, bacteria and viruses. Important viral copathogens include the respiratory syncytial virus, rhinovirus/enterovirus, influenza A and B viruses (IAV and IBV), metapneumovirus, parainfluenza virus, human immunodeficiency virus (HIV), cytomegalovirus, dengue virus, hepatitis B virus, Epstein-Barr virus and other coronaviruses, among which the rhinovirus/enterovirus and IAV are the most common copathogens [5]. Disease progression and outcome in SARS-CoV-2 infection are highly dependent on the host immune response, particularly in the elderly in whom immunosenescence may predispose them to increased risk of coinfection [6]. Immunosenescence renders vaccination less effective and increases the susceptibility to viral infections [7].

Human T-cell lymphotropic virus type-I (HTLV-I) is a single-stranded RNA virus that infects essential human system immune cells, $CD4^+$ T cells. $CD4^+$ T cells are considered "helper" cells because they do not neutralize infections, but rather trigger the body's response to infections [8]. They are considered essential in the activation and growth of cytotoxic T lymphocytes (CTLs). The role of CTLs is to destroy cells infected with microorganisms, such as bacteria or viruses. HTLV-I can cause immune dysfunction even in asymptomatic carriers [3]. HTLV-I can lead to two diseases: adult T-cell leukemia (ATL) and HTLV-I-associated myelopathy/tropical spastic paraparesis (HAM/TSP) [9]. Although HTLV-I can cause fatal diseases (ATL and HAM/TSP), most of the infected persons remain asymptomatic throughout their lives [3]. An estimation by the WHO stated that about 5 to 10 million individuals are infected with HTLV-I worldwide [10]. The primary method of HTLV-I transmission is through bodily fluids including semen, blood and breast milk [11]. In [3,12], two cases of COVID-19 patients with HTLV-I infection have been reported. These reports highlighted the need for the accumulation of similar cases to illustrate the risk factors for severe illness, the best-in-class antiviral agent, the way to manage and prevent secondary infection and the optimal treatment strategy for patients with SARS-CoV-2-HTLV-I coinfection.

Over the years, mathematical models have demonstrated their ability to provide useful insight to gain a further understanding of virus dynamics within the host. These models may assist in the development of viral therapies, as well as in the selection of appropriate therapeutic approaches. Stability analysis of the model's equilibria may help researchers to establish the conditions that ensure the persistence or termination of this infection. Mathematical models of SARS-CoV-2 mono-infection within a host have recently been developed in several works. Hernandez-Vargas and Velasco-Hernandez [13] presented the following SARS-CoV-2 mono-infection model with limited target cells:

$$\dot{X} = -\overbrace{\rho VX}^{\text{SARS-CoV-2 infectious transmission}}, \tag{1.1}$$

$$\dot{N} = \overbrace{\rho VX}^{\text{SARS-CoV-2 infectious transmission}} - \overbrace{\kappa N}^{\text{latent activation}}, \tag{1.2}$$

$$\dot{Y} = \overbrace{\kappa N}^{\text{latent activation}} - \overbrace{\xi_Y Y}^{\text{death}}, \tag{1.3}$$

$$\dot{V} = \overbrace{\eta Y}^{\text{generation of SARS-CoV-2}} - \overbrace{\xi_V V}^{\text{death}}, \tag{1.4}$$

where $X = X(t)$, $N = N(t)$, $Y = Y(t)$ and $V = V(t)$ are the concentrations of uninfected epithelial cells, latently SARS-CoV-2-infected epithelial cells, actively SARS-CoV-2-infected epithelial cells and free SARS-CoV-2 particles at time t, respectively. Li et al. [14] have considered a SARS-CoV-2 infection model with constant regeneration and death for the uninfected epithelial cells:

$$\dot{X} = \delta - \xi_X X - \rho VX.$$

Models presented in [13, 14] have been extended and modified by including (i) latently infected epithelial cells [13,15–17], (ii) the effects of the immune response [18–22], (iii) the effects of different drug therapies [16,23,24] and (iv) the effects of time delay [25].

In very recent works, mathematical models have been formulated to describe the coinfection of COVID-19 with other diseases in epidemiology, such as COVID-19/Dengue [26], COVID-19/Influenza [27], COVID-19/HIV [28], COVID-19/ZIKV [29], COVID-19/Dengue/HIV [30], COVID-19/Tuberculosis [31] and COVID-19/Bacterial [32]. On the other hand, some studies have been devoted to modeling the within-host co-dynamics of COVID-19 with other diseases, including COVID-19/cancer [33], COVID-19/Bacteria [34], COVID-19/HIV [35,36], COVID-19/malaria [37,38] and COVID-19/Influenza [39, 40].

Stability analysis for models describing the within-host dynamics of SARS-CoV-2 infection was studied in [19–21,36,39,41]. Hattaf and Yousfi [19] studied a within-host SARS-CoV-2 infection model with cell-to-cell transmission and CTL immune response. The model included both lytic and nonlytic immune responses. The Lyapunov method was used to prove the global stability of the three equilibria of the model. A SARS-CoV-2 infection model with both CTL and antibody immunities was developed and analyzed in [21]. Mathematical analysis of the model presented in [14] was studied in [41]. Both local and global stability analyses of the model's equilibria were established. Almocera et al. [20] studied the stability of the two-dimensional SARS-CoV-2 dynamics model with an immune response presented in [13]. Elaiw et al. [25] studied the global stability of a delayed SARS-CoV-2 dynamics model with logistic growth of the uninfected epithelial cells and antibody immunity. In very recent works, the Lyapunov method was used to establish the global stability of coinfection models, including SARS-CoV-2/HIV-1 [35,36], SARS-CoV-2/IAV [39] and SARS-CoV-2/malaria [37,38].

During the last decades, modeling and analysis of HTLV-I mono-infection have attracted the interest of several researchers. Stilianakis and Seydel [42] constructed an HTLV-I model within a host as follows:

$$\dot{U} = \overbrace{\gamma}^{\text{CD4}^+\text{T cells production}} - \overbrace{\xi_U U}^{\text{death}} - \overbrace{\pi AU}^{\text{HTLV-I infectious transmission}},$$

$$\dot{L} = \overbrace{\pi AU}^{\text{HTLV-I infectious transmission}} - \overbrace{\alpha L}^{\text{latent activation}} - \overbrace{\xi_L L}^{\text{death}},$$

$$\dot{A} = \overbrace{\alpha L}^{\text{latent activation}} - \overbrace{\vartheta A}^{\text{conversion to ATL}} - \overbrace{\xi_A^* A}^{\text{death}},$$

$$\dot{Z} = \overbrace{\vartheta A}^{\text{conversion to ATL}} + \overbrace{\ell Z\left(1 - \frac{Z}{Z_{\max}}\right)}^{\text{proliferation of ATL}} - \overbrace{\xi_Z Z}^{\text{death}},$$

where $(U, L, A, Z) = (U(t), L(t), A(t), Z(t))$ respectively denotes the concentrations of healthy (or uninfected) CD4$^+$T cells, latently HTLV-I-infected CD4$^+$T cells, actively HTLV-I-infected CD4$^+$T cells and ATL cells. Some biological factors have been considered in the HTLV-I mathematical models by incorporating (i) CTL immunity [9,43–45], (ii) the mitotic transmission of actively infected cells [46–50], (iii) intracellular time delay [51,52] or immune response delay [43, 53] and (iv) reaction and diffusion [54]. Elaiw et al. [55] developed and analyzed a general HTLV-I with CTL immunity, mitosis and time delay. HIV-1 and HTLV-I have similar ways of transmission between individuals. Therefore, we presented and analyzed some models for within-host HIV-1/HTLV-I coinfection [56, 57].

To the best of our knowledge, mathematical modeling of within-host SARS-CoV-2-HTLV-I coinfection has not been studied before. The objective of this work is to formulate a new model for within-host SARS-CoV-2-HTLV-I coinfection. We study the properties of the model's solutions, calculate all equilibrium points, investigate the global stability of equilibria and conduct some numerical simulations.

The SARS-CoV-2/HTLV-I coinfection model presented in this paper can be helpful to describe the co-dynamics of several human viruses. In addition, the model may be used to predict new treatment regimens and strategies for patients who are coinfected with different viruses or multi-variants of a virus [58].

2. Mathematical SARS-CoV-2 and HTLV-I coinfection model

The dynamics of SARS-CoV-2-HTLV-I coinfection is schematically shown in the transfer diagram given in Figure 1. Now, we propose a new ordinary differential equation model for SARS-CoV-2-HTLV-I coinfection within a host as follows:

$$\dot{X} = \delta - \xi_X X - \rho V X, \tag{2.1}$$

$$\dot{N} = \rho V X - (\kappa + \xi_N) N, \tag{2.2}$$

$$\dot{Y} = \kappa N - \xi_Y Y - \mu Y U, \tag{2.3}$$

$$\dot{V} = \eta Y - \xi_V V, \tag{2.4}$$

$$\dot{U} = \gamma + \theta Y U - \xi_U U - \pi A U, \tag{2.5}$$

$$\dot{L} = \pi A U + \omega \varepsilon^* A - (\alpha + \xi_L) L, \tag{2.6}$$

$$\dot{A} = \alpha L + (1 - \omega) \varepsilon^* A - \xi_A^* A. \tag{2.7}$$

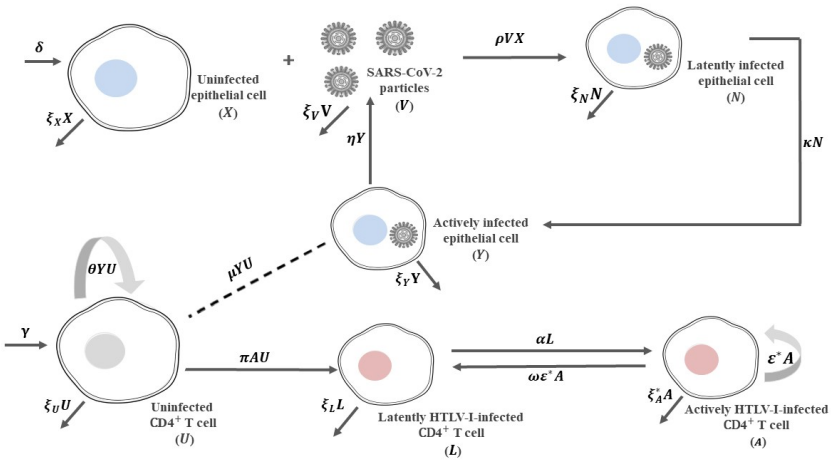

Figure 1. Schematic diagram of the SARS-CoV-2 and HTLV-I coinfection dynamics in vivo.

All parameters of the model described by (2.1)–(2.7) are positive. Since the CD4$^+$T cells help CTLs to kill the actively SARS-CoV-2-infected epithelial cells, we assume implicitly that the actively SARS-CoV-2-infected epithelial cells are killed at a rate μYU and the CD4$^+$T cells are proliferated at a rate θYU. We assume that actively HTLV-I-infected cells proliferate at a rate $\varepsilon^* A$, with a part $\omega\varepsilon^* A$ turning into latent, where $\omega \in (0, 1)$. All parameters of the model are positive. In [49, 56], it was proposed that $\varepsilon^* < \min\{\xi_U, \xi_L, \xi_A^*\}$. Since $0 < \omega < 1$ and $\varepsilon^* < \xi_A^*$, $(1-\omega)\varepsilon^* < \xi_A^*$. Denote $\xi_A = \xi_A^* - (1-\omega)\varepsilon^* > 0$ and $\varepsilon = \omega\varepsilon^*$. Therefore, the model described by (2.1)–(2.7) becomes

$$\dot{X} = \delta - \xi_X X - \rho VX, \tag{2.8}$$
$$\dot{N} = \rho VX - (\kappa + \xi_N)N, \tag{2.9}$$
$$\dot{Y} = \kappa N - \xi_Y Y - \mu YU, \tag{2.10}$$
$$\dot{V} = \eta Y - \xi_V V, \tag{2.11}$$
$$\dot{U} = \gamma + \theta YU - \xi_U U - \pi AU, \tag{2.12}$$
$$\dot{L} = \pi AU + \varepsilon A - (\alpha + \xi_L) L, \tag{2.13}$$
$$\dot{A} = \alpha L - \xi_A A. \tag{2.14}$$

We have $\xi_A - \varepsilon = \xi_A^* - \varepsilon^* > 0$.

Remark 2.1. *If HTLV-I does not exist and we neglect the regeneration of the uninfected epithelial cells, the death of the uninfected epithelial cells and the death of the latently SARS-CoV-2-infected epithelial cells, then the model described by (2.8)–(2.14) will lead to the model described by (1.1)–(1.4). Moreover, in the absence of SARS-CoV-2, then the model described by (2.8)–(2.14) leads to the HTLV-I mono-infection models (without considering the HTLV-I-specific CTL) presented in [49,50].*

3. Properties of solutions

Let $M_i > 0$, $i = 1, 2, 3$ be defined as

$$M_1 = \frac{\delta}{\sigma} + \frac{\mu\gamma}{\sigma\theta},\ M_2 = \frac{2\eta}{\xi_Y} M_1 \text{ and } M_3 = \frac{\theta}{\mu} M_1.$$

Additionally, define the following compact set:

$$\Omega = \{(X, N, Y, V, U, L, A) \in \mathbb{R}^7_{\geq 0} : 0 \leq X, N, Y \leq M_1,\ 0 \leq V \leq M_2,\ 0 \leq U, L, A \leq M_3\}.$$

Lemma 3.1. *The compact set* Ω *is positively invariant for the model described by (2.8)–(2.14).*

Proof. We have that

$$\begin{aligned}
&\dot{X}\,|_{X=0} = \delta > 0, && \dot{N}\,|_{N=0} = \rho VX \geq 0 \text{ for all } X, V \geq 0,\\
&\dot{Y}\,|_{Y=0} = \kappa N \geq 0 \text{ for all } N \geq 0, && \dot{V}\,|_{V=0} = \eta Y \geq 0 \text{ for all } Y \geq 0,\\
&\dot{U}\,|_{U=0} = \gamma > 0, && \dot{L}\,|_{L=0} = \pi AU + \varepsilon A \geq 0 \text{ for all } U, A \geq 0,\\
&\dot{A}\,|_{A=0} = \alpha L \geq 0 \text{ for all } L \geq 0.
\end{aligned}$$

It follows from Proposition B.7 of [59] that $(X(t), N(t), Y(t), V(t), U(t), L(t), A(t)) \in \mathbb{R}^7_{\geq 0}$ for all $t \geq 0$ whenever $(X(0), N(0), Y(0), V(0), U(0), L(0), A(0)) \in \mathbb{R}^7_{\geq 0}$.

To investigate the boundedness of the model's solutions, we define

$$\Gamma(t) = X + N + Y + \frac{\xi_Y}{2\eta} V + \frac{\mu}{\theta}(U + L + A).$$

Then,

$$\dot{\Gamma}(t) = \delta + \frac{\mu}{\theta}\gamma - \xi_X X - \xi_N N - \frac{\xi_Y}{2} Y - \frac{\xi_Y \xi_V}{2\eta} V - \frac{\mu \xi_U}{\theta} U - \frac{\mu \xi_L}{\theta} L - \frac{\mu(\xi_A - \varepsilon)}{\theta} A.$$

We have $\xi_A - \varepsilon = \xi_A^* - \varepsilon^* > 0$. Hence,

$$\begin{aligned}
\dot{\Gamma}(t) &= \delta + \frac{\mu}{\theta}\gamma - \xi_X X - \xi_N N - \frac{\xi_Y}{2} Y - \frac{\xi_Y \xi_V}{2\eta} V - \frac{\mu \xi_U}{\theta} U - \frac{\mu \xi_L}{\theta} L - \frac{\mu\left(\xi_A^* - \varepsilon^*\right)}{\theta} A\\
&\leq \left(\delta + \frac{\mu}{\theta}\gamma\right) - \sigma\left[X + N + Y + \frac{\xi_Y}{2\eta} V + \frac{\mu}{\theta}(U + L + A)\right] = \left(\delta + \frac{\mu}{\theta}\gamma\right) - \sigma\Gamma(t),
\end{aligned}$$

where $\sigma = \min\left\{\xi_X, \xi_N, \frac{\xi_Y}{2}, \xi_V, \xi_U, \xi_L, \xi_A^* - \varepsilon^*\right\}$. Thus, $0 \leq \Gamma(t) \leq M_1$ if $\Gamma(0) \leq M_1$ for $t \geq 0$. Since X, N, Y, V, U, L and A are all non-negative, then $0 \leq X(t), N(t), Y(t) \leq M_1$, $0 \leq V(t) \leq M_2$ and $0 \leq U(t), L(t), A(t) \leq M_3$ for all $t \geq 0$ if $X(0) + N(0) + Y(0) + \frac{\xi_Y}{2\eta} V(0) + \frac{\mu}{\theta}(U(0) + L(0) + A(0)) \leq M_1$. Consequently, $X(t), N(t), Y(t), V(t), U(t), L(t)$ and $A(t)$ are all bounded. □

4. Equilibrium points

To calculate the equilibrium points of the system given by (2.8)–(2.14), we solve the following system:

$$\begin{aligned}
0 &= \delta - \xi_X X - \rho VX,\\
0 &= \rho VX - (\kappa + \xi_N) N,\\
0 &= \kappa N - \xi_Y Y - \mu YU,\\
0 &= \eta Y - \xi_V V,\\
0 &= \gamma + \theta YU - \xi_U U - \pi AU,
\end{aligned}$$

$$0 = \pi AU + \varepsilon A - (\alpha + \xi_L) L,$$
$$0 = \alpha L - \xi_A A.$$

We find that the system admits four equilibrium points.

(i) Uninfected equilibrium point, $EP_0 = (X_0, 0, 0, 0, U_0, 0, 0)$, where $X_0 = \frac{\delta}{\xi_X}$ and $U_0 = \frac{\gamma}{\xi_U}$.

(ii) HTLV-I mono-infection equilibrium point, $EP_1 = (X_1, 0, 0, 0, U_1, L_1, A_1)$, where

$$X_1 = X_0 = \frac{\delta}{\xi_X}, \qquad U_1 = \frac{\xi_L \xi_A + \alpha(\xi_A - \varepsilon)}{\alpha\pi} = \frac{U_0}{R_1},$$
$$L_1 = \frac{\xi_U \xi_A}{\pi\alpha}\left[\frac{\alpha\gamma\pi}{\xi_U(\xi_L\xi_A + \alpha(\xi_A - \varepsilon))} - 1\right] = \frac{\xi_U\xi_A}{\pi\alpha}(R_1 - 1),$$
$$A_1 = \frac{\xi_U}{\pi}\left[\frac{\alpha\gamma\pi}{\xi_U(\xi_L\xi_A + \alpha(\xi_A - \varepsilon))} - 1\right] = \frac{\xi_U}{\pi}(R_1 - 1),$$

where $R_1 = \frac{\alpha\gamma\pi}{\xi_U(\xi_L\xi_A + \alpha(\xi_A - \varepsilon))}$. Here, R_1 is the basic reproduction number of HTLV-I mono-infection. It determines the establishment of HTLV-I infection. Clearly, X_1 is always positive. Also, since $\xi_A - \varepsilon > 0$, U_1 and R_1 are always positive, while L_1 and A_1 are positive if $R_1 > 1$. Therefore, EP_1 exists when $R_1 > 1$.

(iii) SARS-CoV-2 mono-infection equilibrium point, $EP_2 = (X_2, N_2, Y_2, V_2, U_2, 0, 0)$, where

$$Y_2 = \frac{\xi_V}{\eta}V_2, \quad U_2 = \frac{\eta\gamma}{\eta\xi_U - \theta\xi_V V_2}, \quad X_2 = \frac{(\kappa + \xi_N)(Y_2\xi_Y + U_2Y_2\mu)}{\kappa\rho V_2}, \quad N_2 = \frac{Y_2\xi_Y + U_2Y_2\mu}{\kappa}, \tag{4.1}$$

and V_2 satisfies the following equation:

$$\frac{T_1V_2^2 + T_2V_2 + T_3}{\eta\rho\kappa(\eta\xi_U - \theta\xi_V V_2)} = 0, \tag{4.2}$$

where

$$T_1 = \rho\xi_Y\xi_V^2\theta(\kappa + \xi_N),$$
$$T_2 = \xi_X\xi_Y\xi_V^2\theta(\kappa + \xi_N) - \eta\rho\xi_Y\xi_V\xi_U(\kappa + \xi_N) - \eta\rho\gamma\mu\xi_V(\kappa + \xi_N) - \delta\eta\rho\kappa\theta\xi_V,$$
$$T_3 = \delta\eta^2\rho\kappa\xi_U - \eta\xi_X\xi_Y\xi_V\xi_U(\kappa + \xi_N) - \eta\gamma\mu\xi_X\xi_V(\kappa + \xi_N).$$

We want to prove that Eq (4.2) has a positive root. Define a function $F(V)$ as

$$F(V) = \frac{T_1V^2 + T_2V + T_3}{\eta\rho\kappa(\eta\xi_U - \theta\xi_V V)}.$$

We have

$$F(0) = \frac{\delta\eta^2\rho\kappa\xi_U - \eta\xi_X\xi_Y\xi_V\xi_U(\kappa + \xi_N) - \eta\gamma\mu\xi_X\xi_V(\kappa + \xi_N)}{\eta^2\rho\kappa\xi_U} = \frac{\xi_X\xi_V(\kappa + \xi_N)(\xi_Y\xi_U + \gamma\mu)}{\eta\rho\kappa\xi_U}(R_2 - 1),$$

where $R_2 = \frac{\delta\eta\rho\kappa\xi_U}{\xi_X\xi_V(\kappa+\xi_N)(\xi_Y\xi_U+\gamma\mu)}$. This implies that $F(0) > 0$ when $R_2 > 1$. Further,

$$\lim_{V \longrightarrow \frac{\eta\xi_U}{\theta\xi_V}^-} F(V) = -\infty.$$

Furthermore,

$$F'(V) = -\frac{\xi_V(\kappa+\xi_N)}{\kappa\eta\rho\left(\eta\xi_U - V\theta\xi_V\right)^2}\left[\rho\xi_Y\left(V\theta\xi_V - \eta\xi_U\right)^2 + \gamma\mu\xi_X\theta\eta\xi_V + \gamma\mu\rho\eta^2\xi_U\right].$$

Hence, $F'(V) < 0$ for all $V \in (0, \frac{\eta\xi_U}{\theta\xi_V})$. It follows that there exists a unique $V_2 \in (0, \frac{\eta\xi_U}{\theta\xi_V})$ such that $F(V_2) = 0$. From Eq (4.1), we get that $Y_2 > 0$, $U_2 > 0$, $X_2 > 0$ and $N_2 > 0$. As a result, EP_2 exists when $R_2 > 1$. The parameter R_2 represents the basic reproduction number of SARS-CoV-2 mono-infection. It determines the establishment of SARS-CoV-2 mono-infection.

(iv) HTLV-I and SARS-CoV-2 coinfection equilibrium point $EP_3 = (X_3, N_3, Y_3, V_3, U_3, L_3, A_3)$, where

$$\begin{aligned}
X_3 &= \frac{\xi_V(\kappa+\xi_N)\left(\xi_Y\alpha\pi + \mu\left(\xi_L\xi_A + \alpha\left(\xi_A-\varepsilon\right)\right)\right)}{\eta\rho\kappa\alpha\pi},\\
N_3 &= \frac{\xi_X\xi_V\left(\xi_Y\alpha\pi + \mu\left(\xi_L\xi_A + \alpha\left(\xi_A-\varepsilon\right)\right)\right)}{\eta\rho\kappa\alpha\pi}\left[\frac{\delta\eta\rho\kappa\alpha\pi}{\xi_X\xi_V(\kappa+\xi_N)\left(\xi_Y\alpha\pi + \mu\left(\xi_L\xi_A + \alpha\left(\xi_A-\varepsilon\right)\right)\right)} - 1\right],\\
Y_3 &= \frac{\xi_X\xi_V}{\eta\rho}\left[\frac{\delta\eta\rho\kappa\alpha\pi}{\xi_X\xi_V(\kappa+\xi_N)\left(\xi_Y\alpha\pi + \mu\left(\xi_L\xi_A + \alpha\left(\xi_A-\varepsilon\right)\right)\right)} - 1\right],\\
V_3 &= \frac{\xi_X}{\rho}\left[\frac{\delta\eta\rho\kappa\alpha\pi}{\xi_X\xi_V(\kappa+\xi_N)\left(\xi_Y\alpha\pi + \mu\left(\xi_L\xi_A + \alpha\left(\xi_A-\varepsilon\right)\right)\right)} - 1\right],\\
U_3 &= \frac{1}{\alpha\pi}\left(\xi_L\xi_A + \alpha\left(\xi_A-\varepsilon\right)\right),\\
L_3 &= \frac{\xi_A\left(\theta\xi_X\xi_V + \eta\rho\xi_U\right)}{\eta\rho\pi\alpha}\times\\
&\quad\left[\frac{\eta\rho\alpha\pi}{\left(\theta\xi_X\xi_V + \eta\rho\xi_U\right)}\left(\frac{\gamma}{\left(\xi_L\xi_A + \alpha\left(\xi_A-\varepsilon\right)\right)} + \frac{\delta\kappa\theta}{(\kappa+\xi_N)\left(\xi_Y\alpha\pi + \mu\left(\xi_L\xi_A + \alpha\left(\xi_A-\varepsilon\right)\right)\right)}\right) - 1\right],\\
A_3 &= \frac{\left(\theta\xi_X\xi_V + \eta\rho\xi_U\right)}{\eta\rho\pi}\times\\
&\quad\left[\frac{\eta\rho\alpha\pi}{\left(\theta\xi_X\xi_V + \eta\rho\xi_U\right)}\left(\frac{\gamma}{\left(\xi_L\xi_A + \alpha\left(\xi_A-\varepsilon\right)\right)} + \frac{\delta\kappa\theta}{(\kappa+\xi_N)\left(\xi_Y\alpha\pi + \mu\left(\xi_L\xi_A + \alpha\left(\xi_A-\varepsilon\right)\right)\right)}\right) - 1\right].
\end{aligned}$$

It follows that, since $\xi_A - \varepsilon > 0$, X_3 and U_3 are always positive, while $N_3 > 0$, $Y_3 > 0$ and $V_3 > 0$ if $\frac{\delta\eta\rho\kappa\alpha\pi}{\xi_X\xi_V(\kappa+\xi_N)\left(\xi_Y\alpha\pi+\mu\left(\xi_L\xi_A+\alpha\left(\xi_A-\varepsilon\right)\right)\right)} > 1$. On the other hand, $L_3 > 0$ and $A_3 > 0$ when $\frac{\eta\rho\alpha\pi}{\left(\theta\xi_X\xi_V+\eta\rho\xi_U\right)}\left(\frac{\gamma}{\left(\xi_L\xi_A+\alpha\left(\xi_A-\varepsilon\right)\right)} + \frac{\delta\kappa\theta}{(\kappa+\xi_N)\left(\xi_Y\alpha\pi+\mu\left(\xi_L\xi_A+\alpha\left(\xi_A-\varepsilon\right)\right)\right)}\right) > 1$.

Therefore, we can rewrite the components of EP_3 as

$$\begin{aligned}
X_3 &= \frac{X_0}{R_4}, \quad N_3 = \frac{\xi_X\xi_V\left(\xi_Y\alpha\pi + \mu\left(\xi_L\xi_A + \alpha\left(\xi_A-\varepsilon\right)\right)\right)}{\eta\rho\kappa\alpha\pi}\left(R_4-1\right),\\
Y_3 &= \frac{\xi_X\xi_V}{\eta\rho}\left(R_4-1\right), \quad V_3 = \frac{\xi_X}{\rho}\left(R_4-1\right),\\
U_3 &= \frac{1}{\alpha\pi}\left(\xi_L\xi_A + \alpha\left(\xi_A-\varepsilon\right)\right), \quad L_3 = \frac{\xi_A\left(\theta\xi_X\xi_V + \eta\rho\xi_U\right)}{\eta\rho\pi\alpha}\left(R_3-1\right),\\
A_3 &= \frac{\left(\theta\xi_X\xi_V + \eta\rho\xi_U\right)}{\eta\rho\pi}\left(R_3-1\right),
\end{aligned}$$

where

$$R_3 = \frac{\eta\rho\alpha\pi}{\theta\xi_X\xi_V + \eta\rho\xi_U}\left(\frac{\gamma}{(\xi_L\xi_A + \alpha(\xi_A - \varepsilon))} + \frac{\delta\kappa\theta}{(\kappa + \xi_N)(\xi_Y\alpha\pi + \mu(\xi_L\xi_A + \alpha(\xi_A - \varepsilon)))}\right),$$
$$R_4 = \frac{\delta\eta\rho\kappa\alpha\pi}{\xi_X\xi_V(\kappa + \xi_N)(\xi_Y\alpha\pi + \mu(\xi_L\xi_A + \alpha(\xi_A - \varepsilon)))}.$$

Thus, EP_3 exists when $R_3 > 1$ and $R_4 > 1$. At this point, R_3 and R_4 are threshold numbers that determine the occurrence of HTLV-I/SARS-CoV-2 coinfection.

Now, we summarize the above results in the following lemma.

Lemma 4.1. *There exist four threshold numbers R_i, $i = 1, 2, 3, 4$, such that*

(a) if $R_1 \leq 1$, then the uninfected equilibrium point, $EP_0 = (X_0, 0, 0, 0, U_0, 0, 0)$ is the only equilibrium point,

(b) if $R_1 > 1$, then, in addition to EP_0, there is an HTLV-I mono-infection equilibrium point, $EP_1 = (X_1, 0, 0, 0, U_1, L_1, A_1)$,

(c) if $R_2 > 1$, then, in addition to EP_0, there is a SARS-CoV-2 mono-infection equilibrium point, $EP_2 = (X_2, N_2, Y_2, V_2, U_2, 0, 0)$,

(d) if $R_3 > 1$ and $R_4 > 1$, then, in addition to EP_0, there is an HTLV-I and SARS-CoV-2 coinfection equilibrium point, $EP_3 = (X_3, N_3, Y_3, V_3, U_3, L_3, A_3)$.

5. Global stability analysis

In this section, we discuss the global stability of four equilibrium points, EP_i, $i = 0, 1, 2, 3$. We will utilize the following arithmetic-mean–geometric-mean inequality:

$$\frac{\ell_1 + \ell_2 + ... + \ell_n}{n} \geq \sqrt[n]{(\ell_1)(\ell_2)...(\ell_n)}, \quad \ell_i \geq 0, i = 1, 2, ..., n. \tag{5.1}$$

Let Δ_j' be the largest invariant subset of

$$\Delta_j = \left\{(X, N, Y, V, U, L, A) : \frac{d\Phi_j}{dt} = 0\right\}, \quad j = 0, 1, 2, 3,$$

where $\Phi_j(X, N, Y, V, U, L, A)$ is a Lyapunov function candidate.

To prove the results given in the next Theorems 5.1–5.4, we follow the works of [60, 61] to build suitable Lyapunov functions and apply LaSalle's invariance principle [62].

Theorem 5.1. *If $R_1 \leq 1$ and $R_2 \leq 1$, then the uninfected equilibrium point EP_0 is globally asymptotically stable.*

Proof. Define Φ_0 as follows:

$$\Phi_0 = X_0\mathcal{H}\left(\frac{X}{X_0}\right) + N + \frac{\kappa + \xi_N}{\kappa}Y + \frac{\rho X_0}{\xi_V}V + \frac{\mu(\kappa + \xi_N)}{\theta\kappa}U_0\mathcal{H}\left(\frac{U}{U_0}\right)$$
$$+ \frac{\mu(\kappa + \xi_N)}{\theta\kappa}L + \frac{\mu(\kappa + \xi_N)(\alpha + \xi_L)}{\alpha\theta\kappa}A,$$

where $\mathcal{H}(x) = x - 1 - \ln x$.

Obviously, $\Phi_0(X, N, Y, V, U, L, A) > 0$ for all $X, N, Y, V, U, L, A > 0$, while $\Phi_0(X_0, 0, 0, 0, U_0, 0, 0) = 0$. The derivative of Φ_0 with respect to t along the solutions of the system given by (2.8)–(2.14) is calculated as follows:

$$\begin{aligned}
\frac{d\Phi_0}{dt} &= \left(1 - \frac{X_0}{X}\right)\dot{X} + \dot{N} + \frac{\kappa + \xi_N}{\kappa}\dot{Y} + \frac{\rho X_0}{\xi_V}\dot{V} + \frac{\mu(\kappa + \xi_N)}{\theta\kappa}\left(1 - \frac{U_0}{U}\right)\dot{U} + \frac{\mu(\kappa + \xi_N)}{\theta\kappa}\dot{L} \\
&\quad + \frac{\mu(\kappa + \xi_N)(\alpha + \xi_L)}{\alpha\theta\kappa}\dot{A} \\
&= \left(1 - \frac{X_0}{X}\right)(\delta - \xi_X X - \rho V X) + \rho V X - (\kappa + \xi_N)N + \frac{\kappa + \xi_N}{\kappa}(\kappa N - \xi_Y Y - \mu Y U) \\
&\quad + \frac{\rho X_0}{\xi_V}(\eta Y - \xi_V V) + \frac{\mu(\kappa + \xi_N)}{\theta\kappa}\left(1 - \frac{U_0}{U}\right)(\gamma + \theta Y U - \xi_U U - \pi A U) \\
&\quad + \frac{\mu(\kappa + \xi_N)}{\theta\kappa}(\pi A U + \varepsilon A - (\alpha + \xi_L)L) + \frac{\mu(\kappa + \xi_N)(\alpha + \xi_L)}{\alpha\theta\kappa}(\alpha L - \xi_A A) \\
&= \left(1 - \frac{X_0}{X}\right)(\delta - \xi_X X) - \frac{\kappa + \xi_N}{\kappa}\xi_Y Y + \frac{\rho X_0}{\xi_V}\eta Y + \frac{\mu(\kappa + \xi_N)}{\theta\kappa}\left(1 - \frac{U_0}{U}\right)(\gamma - \xi_U U) \\
&\quad - \frac{\mu(\kappa + \xi_N)}{\kappa}Y U_0 + \frac{\mu(\kappa + \xi_N)}{\theta\kappa}\pi A U_0 + \frac{\mu(\kappa + \xi_N)}{\theta\kappa}\varepsilon A - \frac{\mu(\kappa + \xi_N)(\alpha + \xi_L)}{\alpha\theta\kappa}\xi_A A.
\end{aligned}$$

Since $\delta = \xi_X X_0$ and $\gamma = \xi_U U_0$, then

$$\begin{aligned}
\frac{d\Phi_0}{dt} &= -\frac{\xi_X}{X}(X - X_0)^2 + \left(\frac{\rho X_0}{\xi_V}\eta - \frac{\kappa + \xi_N}{\kappa}\xi_Y - \frac{\mu(\kappa + \xi_N)}{\kappa}U_0\right)Y - \frac{\mu(\kappa + \xi_N)}{\theta\kappa}\frac{\xi_U}{U}(U - U_0)^2 \\
&\quad + \frac{\mu(\kappa + \xi_N)}{\theta\kappa}\left(\pi U_0 + \varepsilon - \frac{(\alpha + \xi_L)}{\alpha}\xi_A\right)A \\
&= -\frac{\xi_X}{X}(X - X_0)^2 + \left(\frac{\rho\delta}{\xi_X\xi_V}\eta - \frac{\kappa + \xi_N}{\kappa}\xi_Y - \frac{\mu(\kappa + \xi_N)}{\kappa}\frac{\gamma}{\xi_U}\right)Y - \frac{\mu(\kappa + \xi_N)}{\theta\kappa}\frac{\xi_U}{U}(U - U_0)^2 \\
&\quad + \frac{\mu(\kappa + \xi_N)}{\theta\kappa}\left(\pi\frac{\gamma}{\xi_U} - \frac{\xi_L\xi_A + \alpha(\xi_A - \varepsilon)}{\alpha}\right)A \\
&= -\frac{\xi_X}{X}(X - X_0)^2 + \frac{(\kappa + \xi_N)(\xi_Y\xi_U + \mu\gamma)}{\kappa\xi_U}\left(\frac{\delta\eta\rho\kappa\xi_U}{\xi_X\xi_V(\kappa + \xi_N)(\xi_Y\xi_U + \mu\gamma)} - 1\right)Y \\
&\quad - \frac{\mu(\kappa + \xi_N)}{\theta\kappa}\frac{\xi_U}{U}(U - U_0)^2 + \frac{\mu(\kappa + \xi_N)(\xi_L\xi_A + \alpha(\xi_A - \varepsilon))}{\theta\kappa\alpha}\left(\frac{\pi\alpha\gamma}{\xi_U(\xi_L\xi_A + \alpha(\xi_A - \varepsilon))} - 1\right)A \\
&= -\frac{\xi_X}{X}(X - X_0)^2 + \frac{(\kappa + \xi_N)(\xi_Y\xi_U + \mu\gamma)}{\kappa\xi_U}(R_2 - 1)Y - \frac{\mu(\kappa + \xi_N)}{\theta\kappa}\frac{\xi_U}{U}(U - U_0)^2 \\
&\quad + \frac{\mu(\kappa + \xi_N)(\xi_L\xi_A + \alpha(\xi_A - \varepsilon))}{\theta\kappa\alpha}(R_1 - 1)A.
\end{aligned}$$

Therefore, if $R_1 \leq 1$ and $R_2 \leq 1$, then $\frac{d\Phi_0}{dt} \leq 0$ for all $X, Y, U, A > 0$ and $\frac{d\Phi_0}{dt} = 0$ when $X = X_0$, $U = U_0$ and $Y = A = 0$. The solutions of the system given by (2.8)–(2.14) converge to Δ_0', which comprises elements with $X = X_0$, $U = U_0$ and $Y = A = 0$; then, $\dot{Y} = \dot{A} = 0$. Equations (2.10) and (2.14) yield

$$0 = \dot{Y} = \kappa N \quad \Longrightarrow \quad N(t) = 0 \text{ for all } t,$$

$$0 = \dot{A} = \alpha L \quad \Longrightarrow \quad L(t) = 0 \text{ for all } t.$$

Further, Eq (2.9) gives

$$0 = \dot{N} = \rho V X_0 \quad \Longrightarrow \quad V(t) = 0 \text{ for all } t.$$

Therefore, $\Delta_0' = \{EP_0\}$. We deduce from LaSalle's invariance principle that EP_0 is globally asymptotically stable [62]. □

Theorem 5.2. *If $R_1 > 1$ and $R_4 \leq 1$, then the HTLV-I mono-infection equilibrium point EP_1 is globally asymptotically stable.*

Proof. Let Φ_1 be defined as follows:

$$\Phi_1 = X_1\mathcal{H}\left(\frac{X}{X_1}\right) + N + \frac{\kappa+\xi_N}{\kappa}Y + \frac{\rho X_1}{\xi_V}V + \frac{\mu(\kappa+\xi_N)}{\theta\kappa}U_1\mathcal{H}\left(\frac{U}{U_1}\right) + \frac{\mu(\kappa+\xi_N)}{\theta\kappa}L_1\mathcal{H}\left(\frac{L}{L_1}\right) + \frac{\mu(\kappa+\xi_N)(\alpha+\xi_L)}{\alpha\theta\kappa}A_1\mathcal{H}\left(\frac{A}{A_1}\right).$$

Clearly, $\Phi_1(X, N, Y, V, U, L, A) > 0$ for all $X, N, Y, V, U, L, A > 0$ and $\Phi_1(X_1, 0, 0, 0, U_1, L_1, A_1) = 0$. Calculate $\frac{d\Phi_1}{dt}$ as follows:

$$\begin{aligned}
\frac{d\Phi_1}{dt} &= \left(1-\frac{X_1}{X}\right)\dot{X} + \dot{N} + \frac{\kappa+\xi_N}{\kappa}\dot{Y} + \frac{\rho X_1}{\xi_V}\dot{V} + \frac{\mu(\kappa+\xi_N)}{\theta\kappa}\left(1-\frac{U_1}{U}\right)\dot{U} + \frac{\mu(\kappa+\xi_N)}{\theta\kappa}\left(1-\frac{L_1}{L}\right)\dot{L} \\
&\quad + \frac{\mu(\kappa+\xi_N)(\alpha+\xi_L)}{\alpha\theta\kappa}\left(1-\frac{A_1}{A}\right)\dot{A} \\
&= \left(1-\frac{X_1}{X}\right)(\delta-\xi_X X-\rho V X) + \rho V X - (\kappa+\xi_N)N + \frac{\kappa+\xi_N}{\kappa}(\kappa N - \xi_Y Y - \mu Y U) \\
&\quad + \frac{\rho X_1}{\xi_V}(\eta Y - \xi_V V) + \frac{\mu(\kappa+\xi_N)}{\theta\kappa}\left(1-\frac{U_1}{U}\right)(\gamma+\theta Y U - \xi_U U - \pi A U) \\
&\quad + \frac{\mu(\kappa+\xi_N)}{\theta\kappa}\left(1-\frac{L_1}{L}\right)(\pi A U + \varepsilon A - (\alpha+\xi_L)L) + \frac{\mu(\kappa+\xi_N)(\alpha+\xi_L)}{\alpha\theta\kappa}\left(1-\frac{A_1}{A}\right)(\alpha L - \xi_A A) \\
&= \left(1-\frac{X_1}{X}\right)(\delta-\xi_X X) - \frac{\kappa+\xi_N}{\kappa}\xi_Y Y + \frac{\rho X_1}{\xi_V}\eta Y + \frac{\mu(\kappa+\xi_N)}{\theta\kappa}\left(1-\frac{U_1}{U}\right)(\gamma-\xi_U U) \\
&\quad - \frac{\mu(\kappa+\xi_N)}{\kappa}Y U_1 + \frac{\mu(\kappa+\xi_N)}{\theta\kappa}\pi A U_1 - \frac{\mu(\kappa+\xi_N)}{\theta\kappa}\pi A U\frac{L_1}{L} + \frac{\mu(\kappa+\xi_N)}{\theta\kappa}\varepsilon A - \frac{\mu(\kappa+\xi_N)}{\theta\kappa}\varepsilon A\frac{L_1}{L} \\
&\quad + \frac{\mu(\kappa+\xi_N)}{\theta\kappa}(\alpha+\xi_L)L_1 - \frac{\mu(\kappa+\xi_N)(\alpha+\xi_L)}{\theta\kappa}L\frac{A_1}{A} \\
&\quad - \frac{\mu(\kappa+\xi_N)(\alpha+\xi_L)}{\alpha\theta\kappa}\xi_A A + \frac{\mu(\kappa+\xi_N)(\alpha+\xi_L)}{\alpha\theta\kappa}\xi_A A_1 \\
&= \left(1-\frac{X_1}{X}\right)(\delta-\xi_X X) + \left(\frac{\rho X_1}{\xi_V}\eta - \frac{\kappa+\xi_N}{\kappa}\xi_Y - \frac{\mu(\kappa+\xi_N)}{\kappa}U_1\right)Y \\
&\quad + \frac{\mu(\kappa+\xi_N)}{\theta\kappa}\left(1-\frac{U_1}{U}\right)(\gamma-\xi_U U) + \frac{\mu(\kappa+\xi_N)}{\theta\kappa}\pi A_1 U_1\frac{A}{A_1} - \frac{\mu(\kappa+\xi_N)}{\theta\kappa}\pi A_1 U_1\frac{A U L_1}{A_1 U_1 L} \\
&\quad + \frac{\mu(\kappa+\xi_N)}{\theta\kappa}\varepsilon A_1\frac{A}{A_1} - \frac{\mu(\kappa+\xi_N)}{\theta\kappa}\varepsilon A_1\frac{A L_1}{A_1 L} + \frac{\mu(\kappa+\xi_N)}{\theta\kappa}(\alpha+\xi_L)L_1 \\
&\quad - \frac{\mu(\kappa+\xi_N)(\alpha+\xi_L)}{\theta\kappa}L_1\frac{L A_1}{L_1 A} - \frac{\mu(\kappa+\xi_N)(\alpha+\xi_L)}{\alpha\theta\kappa}\xi_A A_1\frac{A}{A_1} + \frac{\mu(\kappa+\xi_N)(\alpha+\xi_L)}{\alpha\theta\kappa}\xi_A A_1.
\end{aligned}$$

Utilizing the equilibrium point conditions for EP_1:

$$\begin{aligned} \delta &= \xi_X X_1, & \gamma &= \xi_U U_1 + \pi A_1 U_1, \\ \pi A_1 U_1 &= (\alpha + \xi_L) L_1 - \varepsilon A_1, & \alpha L_1 &= \xi_A A_1; \end{aligned}$$

we obtain

$$\begin{aligned} \frac{d\Phi_1}{dt} &= -\frac{\xi_X}{X}(X - X_1)^2 + \left(\frac{\rho X_1}{\xi_V}\eta - \frac{\kappa + \xi_N}{\kappa}\xi_Y - \frac{\mu(\kappa + \xi_N)}{\kappa}U_1\right)Y - \frac{\mu(\kappa + \xi_N)}{\theta\kappa}\frac{\xi_U}{U}(U - U_1)^2 \\ &+ \frac{\mu(\kappa + \xi_N)}{\theta\kappa}\left(1 - \frac{U_1}{U}\right)\pi A_1 U_1 + \frac{\mu(\kappa + \xi_N)}{\theta\kappa}\pi A_1 U_1 \frac{A}{A_1} - \frac{\mu(\kappa + \xi_N)}{\theta\kappa}\pi A_1 U_1 \frac{AUL_1}{A_1 U_1 L} \\ &+ \frac{\mu(\kappa + \xi_N)}{\theta\kappa}\varepsilon A_1 \frac{A}{A_1} - \frac{\mu(\kappa + \xi_N)}{\theta\kappa}\varepsilon A_1 \frac{AL_1}{A_1 L} + \frac{\mu(\kappa + \xi_N)}{\theta\kappa}(\pi A_1 U_1 + \varepsilon A_1) \\ &- \frac{\mu(\kappa + \xi_N)}{\theta\kappa}(\pi A_1 U_1 + \varepsilon A_1)\frac{LA_1}{L_1 A} - \frac{\mu(\kappa + \xi_N)}{\theta\kappa}(\pi A_1 U_1 + \varepsilon A_1)\frac{A}{A_1} + \frac{\mu(\kappa + \xi_N)}{\theta\kappa}(\pi A_1 U_1 + \varepsilon A_1) \\ &= -\frac{\xi_X}{X}(X - X_1)^2 - \frac{\mu(\kappa + \xi_N)}{\theta\kappa}\frac{\xi_U}{U}(U - U_1)^2 \\ &+ \left(\frac{\rho\delta}{\xi_X \xi_V}\eta - \frac{\kappa + \xi_N}{\kappa}\xi_Y - \frac{\mu(\kappa + \xi_N)}{\kappa\alpha\pi}(\xi_L\xi_A + \alpha(\xi_A - \varepsilon))\right)Y \\ &+ \frac{\mu(\kappa + \xi_N)}{\theta\kappa}\pi A_1 U_1\left(3 - \frac{U_1}{U} - \frac{AUL_1}{A_1 U_1 L} - \frac{LA_1}{L_1 A}\right) + \frac{\mu(\kappa + \xi_N)}{\theta\kappa}\varepsilon A_1\left(2 - \frac{AL_1}{A_1 L} - \frac{LA_1}{L_1 A}\right) \\ &= -\frac{\xi_X}{X}(X - X_1)^2 - \frac{\mu(\kappa + \xi_N)}{\theta\kappa}\frac{\xi_U}{U}(U - U_1)^2 \\ &+ \frac{(\kappa + \xi_N)\left[\xi_Y\alpha\pi + \mu(\xi_L\xi_A + \alpha(\xi_A - \varepsilon))\right]}{\kappa\alpha\pi}\left(\frac{\delta\eta\rho\kappa\alpha\pi}{\xi_X\xi_V(\kappa + \xi_N)\left[\xi_Y\alpha\pi + \mu(\xi_L\xi_A + \alpha(\xi_A - \varepsilon))\right]} - 1\right)Y \\ &+ \frac{\mu(\kappa + \xi_N)}{\theta\kappa}\pi A_1 U_1\left(3 - \frac{U_1}{U} - \frac{AUL_1}{A_1 U_1 L} - \frac{LA_1}{L_1 A}\right) + \frac{\mu(\kappa + \xi_N)}{\theta\kappa}\varepsilon A_1\left(2 - \frac{AL_1}{A_1 L} - \frac{LA_1}{L_1 A}\right). \end{aligned}$$

Finally, we get

$$\begin{aligned} \frac{d\Phi_1}{dt} &= -\frac{\xi_X}{X}(X - X_1)^2 - \frac{\mu(\kappa + \xi_N)}{\theta\kappa}\frac{\xi_U}{U}(U - U_1)^2 \\ &+ \frac{(\kappa + \xi_N)\left[\xi_Y\alpha\pi + \mu(\xi_L\xi_A + \alpha(\xi_A - \varepsilon))\right]}{\kappa\alpha\pi}(R_4 - 1)Y \\ &+ \frac{\mu(\kappa + \xi_N)}{\theta\kappa}\pi A_1 U_1\left(3 - \frac{U_1}{U} - \frac{AUL_1}{A_1 U_1 L} - \frac{LA_1}{L_1 A}\right) \\ &+ \frac{\mu(\kappa + \xi_N)}{\theta\kappa}\varepsilon A_1\left(2 - \frac{AL_1}{A_1 L} - \frac{LA_1}{L_1 A}\right). \end{aligned}$$

Using the inequality of (5.1), we obtain

$$\frac{U_1}{U} + \frac{AUL_1}{A_1 U_1 L} + \frac{LA_1}{L_1 A} \geq 3, \ \forall U, L, A > 0,$$

$$\frac{AL_1}{A_1 L} + \frac{LA_1}{L_1 A} \geq 2, \ \forall L, A > 0.$$

Therefore, if $R_4 \leq 1$, then $\frac{d\Phi_1}{dt} \leq 0$ for all $X, Y, U, L, A > 0$, where $\frac{d\Phi_1}{dt} = 0$ when $X = X_1$, $Y = 0$, $U = U_1$, $L = L_1$ and $A = A_1$. The solutions of the system given by (2.8)–(2.14) are limited to Δ_1', which comprises elements with $X = X_1$, $U = U_1$, $L = L_1$, $A = A_1$ and $Y = 0$; then, $\dot{Y} = 0$. Equation (2.10) yields

$$0 = \dot{Y} = \kappa N \quad \Longrightarrow \quad N(t) = 0 \text{ for all } t.$$

Equation (2.9) gives

$$0 = \dot{N} = \rho V X_1 \quad \Longrightarrow \quad V(t) = 0 \text{ for all } t.$$

Consequently, $\Delta_1' = \{EP_1\}$, and then LaSalle's invariance principle implies that EP_1 is globally asymptotically stable [62]. □

Theorem 5.3. *If $R_2 > 1$ and $R_3 \leq 1$, then the SARS-CoV-2 mono-infection equilibrium point EP_2 is globally asymptotically stable.*

Proof. Define Φ_2 as follows:

$$\begin{aligned}\Phi_2 = {} & X_2\mathcal{H}\left(\frac{X}{X_2}\right) + N_2\mathcal{H}\left(\frac{N}{N_2}\right) + \frac{\kappa+\xi_N}{\kappa}Y_2\mathcal{H}\left(\frac{Y}{Y_2}\right) + \frac{\rho X_2}{\xi_V}V_2\mathcal{H}\left(\frac{V}{V_2}\right) \\ & + \frac{\mu(\kappa+\xi_N)}{\theta\kappa}U_2\mathcal{H}\left(\frac{U}{U_2}\right) + \frac{\mu(\kappa+\xi_N)}{\theta\kappa}L + \frac{\mu(\kappa+\xi_N)(\alpha+\xi_L)}{\alpha\theta\kappa}A.\end{aligned}$$

Clearly, $\Phi_2(X, N, Y, V, U, L, A) > 0$ for all $X, N, Y, V, U, L, A > 0$ and $\Phi_2(X_2, N_2, Y_2, V_2, U_2, 0, 0) = 0$. Calculate $\frac{d\Phi_2}{dt}$ as follows:

$$\begin{aligned}\frac{d\Phi_2}{dt} = {} & \left(1-\frac{X_2}{X}\right)\dot{X} + \left(1-\frac{N_2}{N}\right)\dot{N} + \frac{\kappa+\xi_N}{\kappa}\left(1-\frac{Y_2}{Y}\right)\dot{Y} + \frac{\rho X_2}{\xi_V}\left(1-\frac{V_2}{V}\right)\dot{V} \\ & + \frac{\mu(\kappa+\xi_N)}{\theta\kappa}\left(1-\frac{U_2}{U}\right)\dot{U} + \frac{\mu(\kappa+\xi_N)}{\theta\kappa}\dot{L} + \frac{\mu(\kappa+\xi_N)(\alpha+\xi_L)}{\alpha\theta\kappa}\dot{A} \\ = {} & \left(1-\frac{X_2}{X}\right)(\delta - \xi_X X - \rho V X) + \left(1-\frac{N_2}{N}\right)(\rho V X - (\kappa+\xi_N)N) \\ & + \frac{\kappa+\xi_N}{\kappa}\left(1-\frac{Y_2}{Y}\right)(\kappa N - \xi_Y Y - \mu Y U) + \frac{\rho X_2}{\xi_V}\left(1-\frac{V_2}{V}\right)(\eta Y - \xi_V V) \\ & + \frac{\mu(\kappa+\xi_N)}{\theta\kappa}\left(1-\frac{U_2}{U}\right)(\gamma + \theta Y U - \xi_U U - \pi A U) + \frac{\mu(\kappa+\xi_N)}{\theta\kappa}(\pi A U + \varepsilon A - (\alpha+\xi_L)L) \\ & + \frac{\mu(\kappa+\xi_N)(\alpha+\xi_L)}{\alpha\theta\kappa}(\alpha L - \xi_A A) \\ = {} & \left(1-\frac{X_2}{X}\right)(\delta - \xi_X X) - \rho V X\frac{N_2}{N} + (\kappa+\xi_N)N_2 - (\kappa+\xi_N)N\frac{Y_2}{Y} - \frac{\kappa+\xi_N}{\kappa}\xi_Y Y + \frac{\kappa+\xi_N}{\kappa}\xi_Y Y_2 \\ & + \frac{\kappa+\xi_N}{\kappa}\mu Y_2 U + \frac{\rho X_2}{\xi_V}\eta Y - \frac{\rho X_2}{\xi_V}\eta Y\frac{V_2}{V} + \rho X_2 V_2 + \frac{\mu(\kappa+\xi_N)}{\theta\kappa}\left(1-\frac{U_2}{U}\right)(\gamma - \xi_U U) \\ & - \frac{\mu(\kappa+\xi_N)}{\kappa}Y U_2 + \frac{\mu(\kappa+\xi_N)}{\theta\kappa}\pi A U_2 + \frac{\mu(\kappa+\xi_N)}{\theta\kappa}\varepsilon A - \frac{\mu(\kappa+\xi_N)(\alpha+\xi_L)}{\alpha\theta\kappa}\xi_A A \\ = {} & \left(1-\frac{X_2}{X}\right)(\delta - \xi_X X) - \rho V X\frac{N_2}{N} + (\kappa+\xi_N)N_2 - (\kappa+\xi_N)N\frac{Y_2}{Y} + \frac{(\kappa+\xi_N)}{\kappa}\xi_Y Y_2 \\ & + \left(\frac{\rho X_2}{\xi_V}\eta - \frac{\kappa+\xi_N}{\kappa}\xi_Y - \frac{\mu(\kappa+\xi_N)}{\kappa}U_2\right)Y + \frac{(\kappa+\xi_N)}{\kappa}\mu Y_2 U - \frac{\rho X_2}{\xi_V}\eta Y\frac{V_2}{V} + \rho X_2 V_2\end{aligned}$$

$$+\frac{\mu(\kappa+\xi_N)}{\theta\kappa}\left(1-\frac{U_2}{U}\right)(\gamma-\xi_U U)+\frac{\mu(\kappa+\xi_N)}{\theta\kappa}\pi A U_2+\frac{\mu(\kappa+\xi_N)}{\theta\kappa}\varepsilon A-\frac{\mu(\kappa+\xi_N)(\alpha+\xi_L)}{\alpha\theta\kappa}\xi_A A.$$

Utilizing the equilibrium point conditions for EP_2:

$$\begin{aligned}\delta &= \xi_X X_2+\rho V_2 X_2,\\ \rho V_2 X_2 &= (\kappa+\xi_N)N_2,\\ \kappa N_2 &= \xi_Y Y_2+\mu Y_2 U_2,\\ \eta Y_2 &= \xi_V V_2,\\ \gamma &= \xi_U U_2-\theta Y_2 U_2;\end{aligned}$$

we obtain

$$\begin{aligned}\frac{d\Phi_2}{dt} &= -\frac{\xi_X}{X}(X-X_2)^2+\rho V_2X_2-\rho V_2X_2\frac{X_2}{X}-\rho V_2X_2\frac{VXN_2}{V_2X_2N}+\rho V_2X_2-\rho V_2X_2\frac{NY_2}{N_2Y}\\ &+\rho V_2X_2-\frac{(\kappa+\xi_N)}{\kappa}\mu Y_2U_2+\frac{(\kappa+\xi_N)}{\kappa}\mu Y_2U_2\frac{U}{U_2}-\rho V_2X_2\frac{YV_2}{Y_2V}+\rho X_2V_2-\frac{\mu(\kappa+\xi_N)}{\theta\kappa}\frac{\xi_U}{U}(U-U_2)^2\\ &-\frac{\mu(\kappa+\xi_N)}{\kappa}Y_2U_2\left(1-\frac{U_2}{U}\right)+\frac{\mu(\kappa+\xi_N)}{\theta\kappa}\left(\pi U_2-\frac{\xi_L\xi_A+\alpha(\xi_A-\varepsilon)}{\alpha}\right)A\\ &=-\frac{\xi_X}{X}(X-X_2)^2+\rho V_2X_2\left(4-\frac{X_2}{X}-\frac{VXN_2}{V_2X_2N}-\frac{NY_2}{N_2Y}-\frac{YV_2}{Y_2V}\right)-\frac{(\kappa+\xi_N)}{\kappa}\mu Y_2U_2\left(2-\frac{U}{U_2}-\frac{U_2}{U}\right)\\ &-\frac{\mu(\kappa+\xi_N)}{\theta\kappa}\frac{\xi_U}{U}(U-U_2)^2+\frac{\mu(\kappa+\xi_N)}{\theta\kappa}\left(\pi U_2-\frac{\xi_L\xi_A+\alpha(\xi_A-\varepsilon)}{\alpha}\right)A.\end{aligned}$$

We have

$$\begin{aligned}&-\frac{\kappa+\xi_N}{\kappa}\mu Y_2U_2\left(2-\frac{U}{U_2}-\frac{U_2}{U}\right)-\frac{\mu(\kappa+\xi_N)}{\theta\kappa}\frac{\xi_U}{U}(U-U_2)^2\\ &=\frac{(\kappa+\xi_N)}{\kappa}\frac{\mu Y_2}{U}(U-U_2)^2-\frac{\mu(\kappa+\xi_N)}{\theta\kappa}\frac{\xi_U}{U}(U-U_2)^2\\ &=\frac{\mu(\kappa+\xi_N)}{\theta\kappa}\frac{(U-U_2)^2}{U}(\theta Y_2-\xi_U)\\ &=-\frac{\mu\gamma(\kappa+\xi_N)}{\theta\kappa UU_2}(U-U_2)^2.\end{aligned}$$

Collecting terms, we get

$$\begin{aligned}\frac{d\Phi_2}{dt} &= -\frac{\xi_X}{X}(X-X_2)^2+\rho V_2X_2\left(4-\frac{X_2}{X}-\frac{VXN_2}{V_2X_2N}-\frac{NY_2}{N_2Y}-\frac{YV_2}{Y_2V}\right)\\ &-\frac{\mu\gamma(\kappa+\xi_N)}{\theta\kappa UU_2}(U-U_2)^2+\frac{\mu(\kappa+\xi_N)}{\theta\kappa}\left(\pi U_2-\frac{\xi_L\xi_A+\alpha(\xi_A-\varepsilon)}{\alpha}\right)A.\end{aligned}$$

Hence, if $R_3\le 1$, then EP_3 does not exist since $A_3\le 0$ and $L_3\le 0$. This implies that

$$\begin{aligned}\dot{A}(t) &= \alpha L-\xi_A A\le 0,\\ \dot{L}(t) &= \pi AU+\varepsilon A-(\alpha+\xi_L)L\le 0.\end{aligned}$$

It follows that $\left(\pi U - \frac{\xi_L\xi_A+\alpha(\xi_A-\varepsilon)}{\alpha}\right)A \leq 0$ for all $A > 0$. Thus, $\pi U_2 - \frac{\xi_L\xi_A+\alpha(\xi_A-\varepsilon)}{\alpha} \leq 0$, and, by using the inequality of (5.1), we obtain

$$\frac{X_2}{X} + \frac{VXN_2}{V_2X_2N} + \frac{NY_2}{N_2Y} + \frac{YV_2}{Y_2V} \geq 4, \ \forall X, N, Y, V > 0.$$

Thus, $\frac{d\Phi_2}{dt} \leq 0$ for all $X, N, Y, V, U, L, A > 0$ and $\frac{d\Phi_2}{dt} = 0$ when $X = X_2$, $N = N_2, Y = Y_2$, $V = V_2$, $U = U_2$ and $A = 0$. The solutions of the system converge to Δ_2', which comprises elements with $A = 0$. It follows that $\dot{A} = 0$, and Eq (2.14) becomes

$$0 = \dot{A} = \alpha L \Longrightarrow L(t) = 0 \text{ for all } t.$$

Therefore, $\Delta_2' = \{EP_2\}$. LaSalle's invariance principle implies that EP_2 is globally asymptotically stable [62].□

Let us define a parameter $\hat{R}$ as follows:

$$\hat{R} = \frac{\eta\rho\alpha\pi\gamma}{(\theta\xi_X\xi_V + \eta\rho\xi_U)(\xi_L\xi_A + \alpha(\xi_A - \varepsilon))}.$$

Theorem 5.4. *If $R_4 > 1$ and $1 < R_3 \leq 1 + \hat{R}$, then the HTLV-I/SARS-CoV-2 coinfection equilibrium point EP_3 is globally asymptotically stable.*

Proof. Define Φ_3 as follows:

$$\begin{aligned}\Phi_3 = {} & X_3\mathcal{H}\left(\frac{X}{X_3}\right) + N_3\mathcal{H}\left(\frac{N}{N_3}\right) + \frac{\kappa+\xi_N}{\kappa}Y_3\mathcal{H}\left(\frac{Y}{Y_3}\right) + \frac{\rho X_3}{\xi_V}V_3\mathcal{H}\left(\frac{V}{V_3}\right) \\ & + \frac{\mu(\kappa+\xi_N)}{\theta\kappa}U_3\mathcal{H}\left(\frac{U}{U_3}\right) + \frac{\mu(\kappa+\xi_N)}{\theta\kappa}L_3\mathcal{H}\left(\frac{L}{L_3}\right) + \frac{\mu(\kappa+\xi_N)(\alpha+\xi_L)}{\alpha\theta\kappa}A_3\mathcal{H}\left(\frac{A}{A_3}\right).\end{aligned}$$

Clearly, $\Phi_3(X, N, Y, V, U, L, A) > 0$ for all $X, N, Y, V, U, L, A > 0$ and $\Phi_3(X_3, N_3, Y_3, V_3, U_3, L_3, A_3) = 0$. Calculate $\frac{d\Phi_3}{dt}$ as follows:

$$\begin{aligned}\frac{d\Phi_3}{dt} = {} & \left(1 - \frac{X_3}{X}\right)\dot{X} + \left(1 - \frac{N_3}{N}\right)\dot{N} + \frac{\kappa+\xi_N}{\kappa}\left(1 - \frac{Y_3}{Y}\right)\dot{Y} + \frac{\rho X_3}{\xi_V}\left(1 - \frac{V_3}{V}\right)\dot{V} \\ & + \frac{\mu(\kappa+\xi_N)}{\theta\kappa}\left(1 - \frac{U_3}{U}\right)\dot{U} + \frac{\mu(\kappa+\xi_N)}{\theta\kappa}\left(1 - \frac{L_3}{L}\right)\dot{L} + \frac{\mu(\kappa+\xi_N)(\alpha+\xi_L)}{\alpha\theta\kappa}\left(1 - \frac{A_3}{A}\right)\dot{A} \\ = {} & \left(1 - \frac{X_3}{X}\right)(\delta - \xi_X X - \rho VX) + \left(1 - \frac{N_3}{N}\right)(\rho VX - (\kappa+\xi_N)N) + \frac{\kappa+\xi_N}{\kappa}\left(1 - \frac{Y_3}{Y}\right)\times \\ & (\kappa N - \xi_Y Y - \mu YU) + \frac{\rho X_3}{\xi_V}\left(1 - \frac{V_3}{V}\right)(\eta Y - \xi_V V) + \frac{\mu(\kappa+\xi_N)}{\theta\kappa}\left(1 - \frac{U_3}{U}\right)(\gamma + \theta YU - \xi_U U - \pi AU) \\ & + \frac{\mu(\kappa+\xi_N)}{\theta\kappa}\left(1 - \frac{L_3}{L}\right)(\pi AU + \varepsilon A - (\alpha+\xi_L)L) + \frac{\mu(\kappa+\xi_N)(\alpha+\xi_L)}{\alpha\theta\kappa}\left(1 - \frac{A_3}{A}\right)(\alpha L - \xi_A A) \\ = {} & \left(1 - \frac{X_3}{X}\right)(\delta - \xi_X X) - \rho VX\frac{N_3}{N} + (\kappa+\xi_N)N_3 - (\kappa+\xi_N)N\frac{Y_3}{Y} - \frac{\kappa+\xi_N}{\kappa}\xi_Y Y + \frac{\kappa+\xi_N}{\kappa}\xi_Y Y_3 \\ & + \frac{\kappa+\xi_N}{\kappa}\mu Y_3 U + \frac{\rho X_3}{\xi_V}\eta Y - \frac{\rho X_3}{\xi_V}\eta Y\frac{V_3}{V} + \rho X_3 V_3 + \frac{\mu(\kappa+\xi_N)}{\theta\kappa}\left(1 - \frac{U_3}{U}\right)(\gamma - \xi_U U) - \frac{\mu(\kappa+\xi_N)}{\kappa}YU_3 \\ & + \frac{\mu(\kappa+\xi_N)}{\theta\kappa}\pi AU_3 - \frac{\mu(\kappa+\xi_N)}{\theta\kappa}\pi AU\frac{L_3}{L} + \frac{\mu(\kappa+\xi_N)}{\theta\kappa}\varepsilon A - \frac{\mu(\kappa+\xi_N)}{\theta\kappa}\varepsilon A\frac{L_3}{L} + \frac{\mu(\kappa+\xi_N)}{\theta\kappa}(\alpha+\xi_L)L_3\end{aligned}$$

$$
\begin{aligned}
&- \frac{\mu(\kappa+\xi_N)(\alpha+\xi_L)}{\theta\kappa} L\frac{A_3}{A} - \frac{\mu(\kappa+\xi_N)(\alpha+\xi_L)}{\alpha\theta\kappa}\xi_A A + \frac{\mu(\kappa+\xi_N)(\alpha+\xi_L)}{\alpha\theta\kappa}\xi_A A_3 \\
&= \left(1-\frac{X_3}{X}\right)(\delta-\xi_X X) - \rho V X\frac{N_3}{N} + (\kappa+\xi_N)N_3 - (\kappa+\xi_N)N\frac{Y_3}{Y} + \frac{\kappa+\xi_N}{\kappa}\xi_Y Y_3 \\
&+ \left(\frac{\rho X_3}{\xi_V}\eta - \frac{\kappa+\xi_N}{\kappa}\xi_Y - \frac{\mu(\kappa+\xi_N)}{\kappa}U_3\right)Y + \frac{\kappa+\xi_N}{\kappa}\mu Y_3 U - \frac{\rho X_3}{\xi_V}\eta Y\frac{V_3}{V} + \rho X_3 V_3 \\
&+ \frac{\mu(\kappa+\xi_N)}{\theta\kappa}\left(1-\frac{U_3}{U}\right)(\gamma-\xi_U U) + \frac{\mu(\kappa+\xi_N)}{\theta\kappa}\pi A U_3 - \frac{\mu(\kappa+\xi_N)}{\theta\kappa}\pi A U\frac{L_3}{L} + \frac{\mu(\kappa+\xi_N)}{\theta\kappa}\varepsilon A \\
&- \frac{\mu(\kappa+\xi_N)}{\theta\kappa}\varepsilon A\frac{L_3}{L} + \frac{\mu(\kappa+\xi_N)}{\theta\kappa}(\alpha+\xi_L)L_3 - \frac{\mu(\kappa+\xi_N)(\alpha+\xi_L)}{\theta\kappa}L\frac{A_3}{A} - \frac{\mu(\kappa+\xi_N)(\alpha+\xi_L)}{\alpha\theta\kappa}\xi_A A \\
&+ \frac{\mu(\kappa+\xi_N)(\alpha+\xi_L)}{\alpha\theta\kappa}\xi_A A_3.
\end{aligned}
$$

Utilizing the equilibrium point conditions for EP_3:

$$
\begin{aligned}
\delta &= \xi_X X_3 + \rho V_3 X_3, \\
\rho V_3 X_3 &= (\kappa+\xi_N)N_3, \\
\kappa N_3 &= \xi_Y Y_3 + \mu Y_3 U_3, \\
\eta Y_3 &= \xi_V V_3, \\
\gamma &= \xi_U U_3 - \theta Y_3 U_3 + \pi A_3 U_3, \\
\pi A_3 U_3 &= (\alpha+\xi_L)L_3 - \varepsilon A_3, \\
\alpha L_3 &= \xi_A A_3;
\end{aligned}
$$

we obtain

$$
\begin{aligned}
\frac{d\Phi_3}{dt} &= -\frac{\xi_X}{X}(X-X_3)^2 + \rho V_3 X_3 - \rho V_3 X_3\frac{X_3}{X} - \rho V_3 X_3\frac{VXN_3}{V_3X_3N} + \rho V_3 X_3 - \rho V_3 X_3\frac{NY_3}{N_3Y} \\
&+ \rho V_3 X_3 - \frac{(\kappa+\xi_N)}{\kappa}\mu Y_3 U_3 + \frac{(\kappa+\xi_N)}{\kappa}\mu Y_3 U_3\frac{U}{U_3} - \rho V_3 X_3\frac{YV_3}{Y_3V} + \rho X_3 V_3 - \frac{\mu(\kappa+\xi_N)}{\theta\kappa}\frac{\xi_U}{U}(U-U_3)^2 \\
&- \frac{\mu(\kappa+\xi_N)}{\kappa}Y_3U_3\left(1-\frac{U_3}{U}\right) + \frac{\mu(\kappa+\xi_N)}{\theta\kappa}\pi A_3U_3\left(1-\frac{U_3}{U}\right) + \frac{\mu(\kappa+\xi_N)}{\theta\kappa}\pi A_3U_3\frac{A}{A_3} \\
&- \frac{\mu(\kappa+\xi_N)}{\theta\kappa}\pi A_3U_3\frac{AUL_3}{A_3U_3L} + \frac{\mu(\kappa+\xi_N)}{\theta\kappa}\varepsilon A_3\frac{A}{A_3} - \frac{\mu(\kappa+\xi_N)}{\theta\kappa}\varepsilon A_3\frac{AL_3}{A_3L} + \frac{\mu(\kappa+\xi_N)}{\theta\kappa}(\pi A_3U_3+\varepsilon A_3) \\
&- \frac{\mu(\kappa+\xi_N)}{\theta\kappa}(\pi A_3U_3+\varepsilon A_3)\frac{LA_3}{L_3A} - \frac{\mu(\kappa+\xi_N)}{\theta\kappa}(\pi A_3U_3+\varepsilon A_3)\frac{A}{A_3} + \frac{\mu(\kappa+\xi_N)}{\theta\kappa}(\pi A_3U_3+\varepsilon A_3) \\
&= -\frac{\xi_X}{X}(X-X_3)^2 + \rho V_3X_3\left(4-\frac{X_3}{X}-\frac{VXN_3}{V_3X_3N}-\frac{NY_3}{N_3Y}-\frac{YV_3}{Y_3V}\right) - \frac{(\kappa+\xi_N)}{\kappa}\mu Y_3U_3\left(2-\frac{U}{U_3}-\frac{U_3}{U}\right) \\
&- \frac{\mu(\kappa+\xi_N)}{\theta\kappa}\frac{\xi_U}{U}(U-U_3)^2 + \frac{\mu(\kappa+\xi_N)}{\theta\kappa}\pi A_3U_3\left(3-\frac{U_3}{U}-\frac{AUL_3}{A_3U_3L}-\frac{LA_3}{L_3A}\right) \\
&+ \frac{\mu(\kappa+\xi_N)}{\theta\kappa}\varepsilon A_3\left(2-\frac{AL_3}{A_3L}-\frac{LA_3}{L_3A}\right).
\end{aligned}
$$

We have

$$
-\frac{(\kappa+\xi_N)}{\kappa}\mu Y_3U_3\left(2-\frac{U}{U_3}-\frac{U_3}{U}\right) - \frac{\mu(\kappa+\xi_N)}{\theta\kappa}\frac{\xi_U}{U}(U-U_3)^2
$$

$$
\begin{aligned}
&= \frac{(\kappa+\xi_N)}{\kappa}\frac{\mu Y_3}{U}(U-U_3)^2 - \frac{\mu(\kappa+\xi_N)}{\theta\kappa}\frac{\xi_U}{U}(U-U_3)^2 \\
&= \frac{\mu(\kappa+\xi_N)}{\kappa}\frac{(U-U_3)^2}{U}\left(Y_3-\frac{\xi_U}{\theta}\right) \\
&= \frac{\mu(\kappa+\xi_N)(\theta\xi_X\xi_V+\eta\rho\xi_U)}{\eta\rho\kappa\theta}\frac{(U-U_3)^2}{U}\left(R_3-\hat{R}-1\right).
\end{aligned}
$$

Collecting terms, we get

$$
\begin{aligned}
\frac{d\Phi_3}{dt} &= -\frac{\xi_X}{X}(X-X_3)^2 + \rho V_3 X_3\left(4-\frac{X_3}{X}-\frac{VXN_3}{V_3X_3N}-\frac{NY_3}{N_3Y}-\frac{YV_3}{Y_3V}\right) \\
&+ \frac{\mu(\kappa+\xi_N)(\theta\xi_X\xi_V+\eta\rho\xi_U)}{\eta\rho\kappa\theta}\frac{(U-U_3)^2}{U}\left(R_3-\hat{R}-1\right) \\
&+ \frac{\mu(\kappa+\xi_N)}{\theta\kappa}\pi A_3U_3\left(3-\frac{U_3}{U}-\frac{AUL_3}{A_3U_3L}-\frac{LA_3}{L_3A}\right) + \frac{\mu(\kappa+\xi_N)}{\theta\kappa}\varepsilon A_3\left(2-\frac{AL_3}{A_3L}-\frac{LA_3}{L_3A}\right).
\end{aligned}
$$

Using the inequality of (5.1), we obtain

$$
\begin{aligned}
\frac{X_3}{X}+\frac{VXN_3}{V_3X_3N}+\frac{NY_3}{N_3Y}+\frac{YV_3}{Y_3V} &\geq 4,\ \forall X,N,Y,V>0, \\
\frac{U_3}{U}+\frac{AUL_3}{A_3U_3L}+\frac{LA_3}{L_3A} &\geq 3,\ \forall U,L,A>0, \\
\frac{AL_3}{A_3L}+\frac{LA_3}{L_3A} &\geq 2,\ \forall L,A>0.
\end{aligned}
$$

Moreover, since $1 < R_3 \leq 1+\hat{R}$, we get $\frac{d\Phi_3}{dt} \leq 0$ for all $X,N,Y,V,U,L,A > 0$ and $\frac{d\Phi_3}{dt} = 0$ when $X = X_3$, $N = N_3$, $Y = Y_3$, $V = V_3$, $U = U_3$, $L = L_3$ and $A = A_3$. The solutions of the system converge to Δ_3'. Clearly, $\Delta_3' = \{EP_3\}$, and then LaSalle's invariance principle implies that EP_3 is globally asymptotically stable [62]. □

Based on the above findings, we summarize the existence and global stability conditions for all equilibrium points in Table 1.

Table 1. Conditions of existence and global stability of the system's equilibria.

Equilibrium point	Existence conditions	Global stability conditions
$EP_0 = (X_0, 0, 0, 0, U_0, 0, 0)$	None	$R_1 \leq 1$ and $R_2 \leq 1$
$EP_1 = (X_1, 0, 0, 0, U_1, L_1, A_1)$	$R_1 > 1$	$R_1 > 1$ and $R_4 \leq 1$
$EP_2 = (X_2, N_2, Y_2, V_2, U_2, 0, 0)$	$R_2 > 1$	$R_2 > 1$ and $R_3 \leq 1$
$EP_3 = (X_3, N_3, Y_3, V_3, U_3, L_3, A_3)$	$R_3 > 1$ and $R_4 > 1$	$R_4 > 1$ and $1 < R_3 \leq 1+\hat{R}$

6. Numerical simulations

In this section, we present some numerical results for the model described by (2.1)–(2.7) to illustrate the stability of equilibrium points. We used the ODE45 solver in MATLAB to solve the system numerically.

6.1. Stability of equilibrium points

We solve the system with three initial conditions:

IC1: $(X(0), N(0), Y(0), V(0), U(0), L(0), A(0)) = (9, 0.0001, 0.0002, 0.0003, 600, 150, 15)$,
IC2: $(X(0), N(0), Y(0), V(0), U(0), L(0), A(0)) = (5, 0.0005, 0.0006, 0.0007, 500, 200, 20)$,
IC3: $(X(0), N(0), Y(0), V(0), U(0), L(0), A(0)) = (1, 0.001, 0.002, 0.003, 400, 250, 25)$.

Table 2. Model parameters.

Parameter	Description	Value	Source
δ	Recruitment rate of uninfected epithelial cells	0.11	[25]
ξ_X	Natural death rate constant of uninfected epithelial cells	0.011	[25]
ρ	Virus-cell incidence rate constant between free SARS-CoV-2 particles and uninfected epithelial cells	Varies	Assumed
κ	Transmission rate constant of latently SARS-CoV-2-infected epithelial cells that become actively SARS-CoV-2-infected epithelial cells	4.08	[35,40]
ξ_N	Death rate constant of latently SARS-CoV-2-infected epithelial cells	0.11	[25]
ξ_Y	Death rate constant of actively SARS-CoV-2-infected epithelial cells	0.11	[35,41]
μ	Killing rate constant of actively SARS-CoV-2-infected epithelial cells due to immune response	Varies	Assumed
η	Generation rate constant of new SARS-CoV-2 particles	0.24	[35,41]
ξ_V	Death rate constant of free SARS-CoV-2 particles	Varies	Assumed
γ	Recruitment rate for the uninfected CD4$^+$T cells	10	[48,49,63]
θ	Proliferation rate constant of uninfected CD4$^+$T cells due to actively SARS-CoV-2-infected epithelial cells	0.1	[35,64]
ξ_U	Natural mortality rate constant for the uninfected CD4$^+$T cells	0.012	[46, 48, 49]
π	Cell-cell incidence rate constant between uninfected CD4$^+$T cells and actively HTLV-I-infected CD4$^+$T cells	Varies	Assumed
ω	Probability of new HTLV-I infections via mitosis could enter a latent period	0.9	[47]
ε^*	Proliferation rate constant of newly HTLV-I-infected CD4$^+$T cells from mitosis	0.011	[47]
α	Transmission rate constant of latently HTLV-I-infected CD4$^+$T cells that become actively HTLV-I-infected CD4$^+$T cells	0.003	[46,48,49,65]
ξ_L	Death rate constant of latently HTLV-I-infected CD4$^+$T cells	0.03	[47–50]
ξ_A^*	Death rate constant of actively HTLV-I-infected CD4$^+$T cells	0.03	[46, 48, 49]

Table 2 contains the values of some parameters. We mention that the values of some parameters of the model are taken from previous studies for SARS-CoV-2 and HTLV-I mono-infections, while other parameters ρ, μ, ξ_V and π are chosen just to conduct the numerical simulations. To the best of our knowledge, now, there is no available data from SARS-CoV-2 and HTLV-I coinfection patients. Therefore, estimation of the parameters of the coinfection model is still open for future investigation. We vary the parameters, ρ, μ, ξ_V and π to obtain four cases, as follows:

Case 1. *($R_1 \leq 1$ and $R_2 \leq 1$): Choose $\rho = 0.8$, $\mu = 1.1$, $\xi_V = 5.5$ and $\pi = 0.0001$, which gives $R_1 = 0.2706 < 1$ and $R_2 = 0.0004 < 1$. Based on Theorem 5.1, the equilibrium point EP_0 is globally asymptotically stable. This is illustrated in Figure 2, where the concentrations of the uninfected epithelial cells and uninfected $CD4^+T$ cells tend to their healthy values $X_0 = 10$ and $U_0 = 833.33$ while the concentrations of the other compartments tend to zero. This case means that there are no SARS-CoV-2 and HTLV-I infections in the body.*

Case 2. *($R_1 > 1$ and $R_4 \leq 1$): We take $\rho = 0.5$, $\mu = 1.1$, $\xi_V = 5.5$ and $\pi = 0.0015$. So, we get $R_1 = 4.0584 > 1$ and $R_4 = 0.0009 < 1$. According to Lemma 4.1 and Theorem 5.2, the HTLV-I mono-infection equilibrium point EP_1 exists and is globally asymptotically stable. Figure 3 shows that the model solutions converge to the equilibrium point $EP_1 = (10, 0, 0, 0, 205.33, 235.7, 24.47)$ for all initials IC1–IC3. In this situation, the patient becomes infected by HTLV-I, while the SARS-CoV-2 infection is cleared.*

Case 3. *($R_2 > 1$ and $R_3 \leq 1$): We choose $\rho = 3$, $\mu = 0.01$, $\xi_V = 0.04$ and $\pi = 0.0001$. Then, we calculate $R_2 = 20.7589 > 1$ and $R_3 = 0.2979 < 1$. Lemma 4.1 and Theorem 5.3 state that the SARS-CoV-2 mono-infection equilibrium point $EP_2 = (0.529, 0.025, 0.011, 0.066, 916.87, 0, 0)$ exists and is globally asymptotically stable. Figure 4 displays the numerical solutions of the system converge to EP_2 for all three initials IC1–IC3. The results support the theoretical results presented in Theorem 5.3. In this situation, the patient becomes infected by SARS-CoV-2, while the HTLV-I infection is removed.*

Case 4. *($R_4 > 1$ and $1 < R_3 \leq 1 + \hat{R}$): We consider $\rho = 3$, $\mu = 0.01$, $\xi_V = 0.6$ and $\pi = 0.0015$. So, we get $R_4 = 5.4014 > 1$, $R_3 = 4.1538 > 1$ and $R_3 < 1 + \hat{R} = 4.7704$. Lemma 4.1 and Theorem 5.4 state that the HTLV-I/SARS-CoV-2 coinfection equilibrium point $EP_3 = (1.85, 0.021, 0.04, 0.016, 205.33, 261.62, 27.16)$ exists and is globally asymptotically stable. Figure 5 shows that the solutions of the system converge to EP_3 for all initials IC1–IC3. The results support the theoretical results presented in Theorem 5.4. In this case, a SARS-CoV-2 and HTLV-I coinfection happens, where an HTLV-I-patient gets contaminated with COVID-19. $CD4^+T$ cells are animated to dispense with SARS-CoV-2 disease from the body. In any case, assuming that the patient has low $CD4^+$ T cell counts, the freedom of SARS-CoV-2 may not be accomplished. This can prompt extreme contamination and passing. Now, we check the local stability of the model's equilibria.*

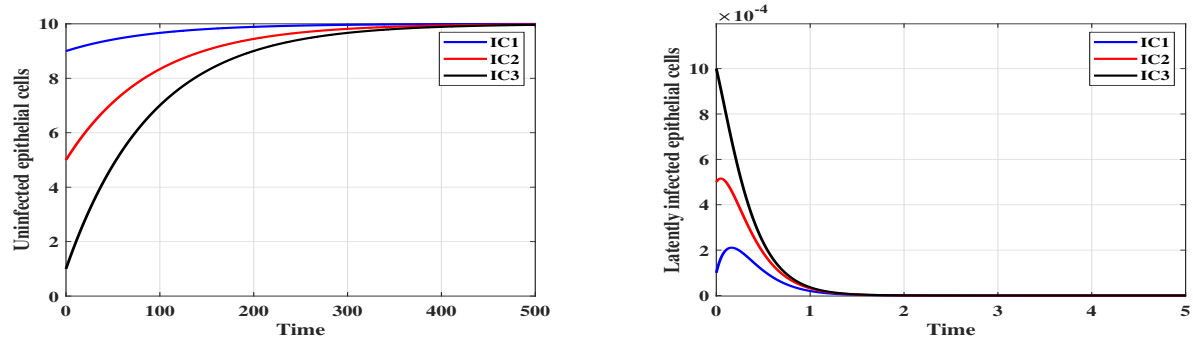

(a) Uninfected epithelial cells

(b) Latently infected epithelial cells

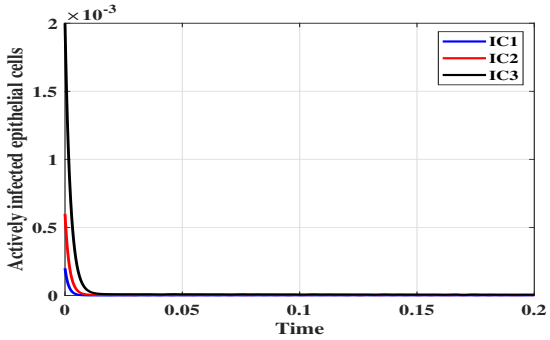

(c) Actively infected epithelial cells

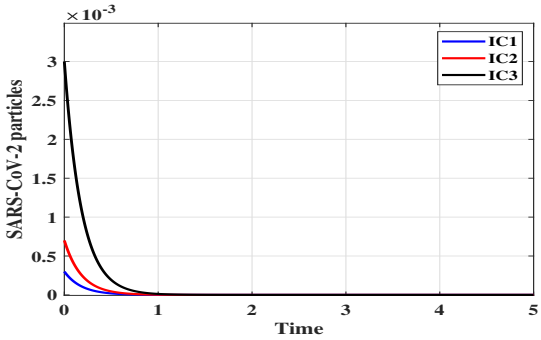

(d) SARS-CoV-2 particles

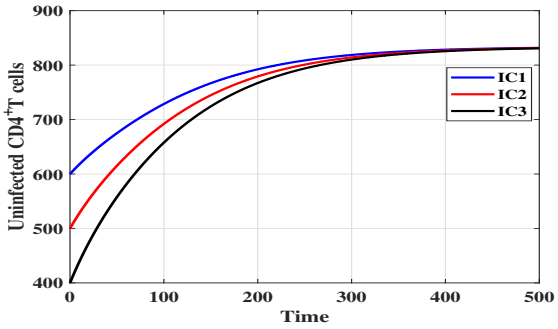

(e) Uninfected CD4$^+$T cells

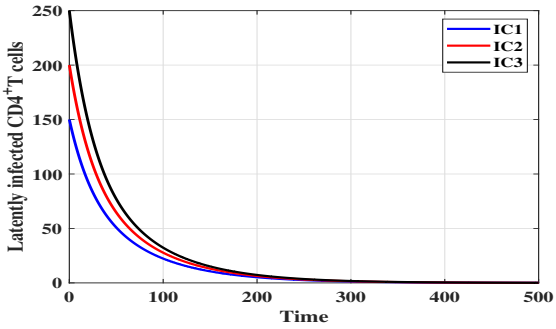

(f) Latently infected CD4$^+$T cells

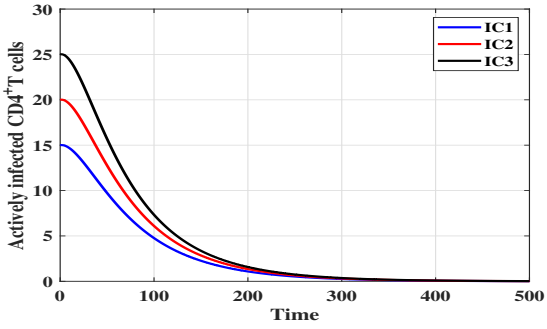

(g) Actively infected CD4$^+$T cells

Figure 2. Solutions of the system described by (2.1)–(2.7) with the initial conditions IC1–IC3 in Case 1.

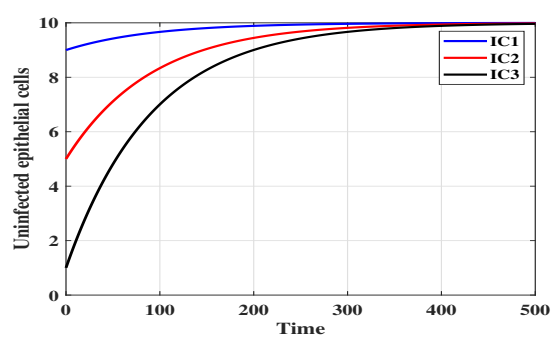

(a) Uninfected epithelial cells

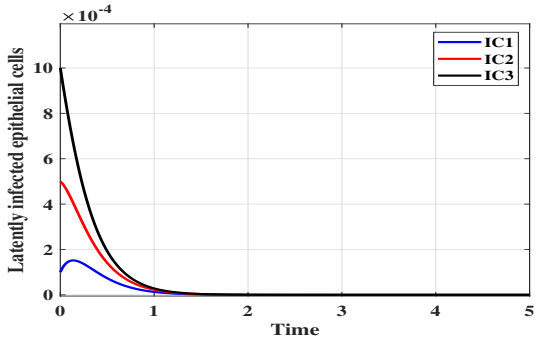

(b) Latently infected epithelial cells

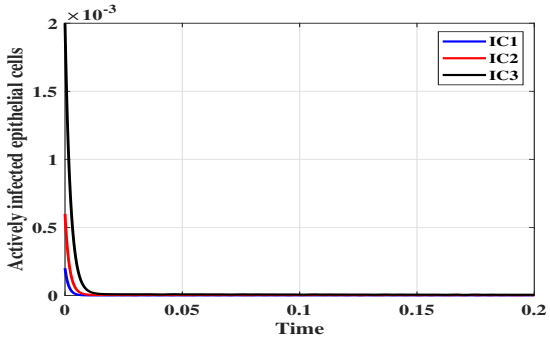

(c) Actively infected epithelial cells

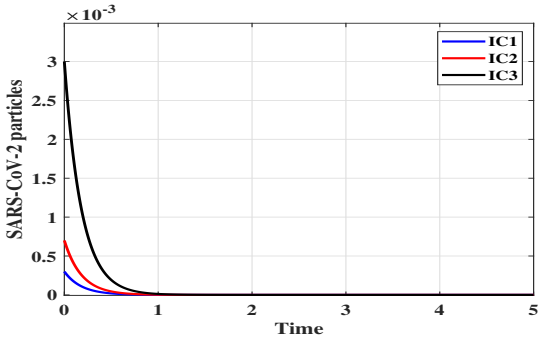

(d) SARS-CoV-2 particles

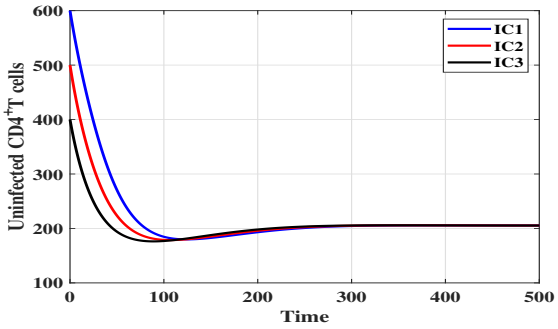

(e) Uninfected CD4$^+$T cells

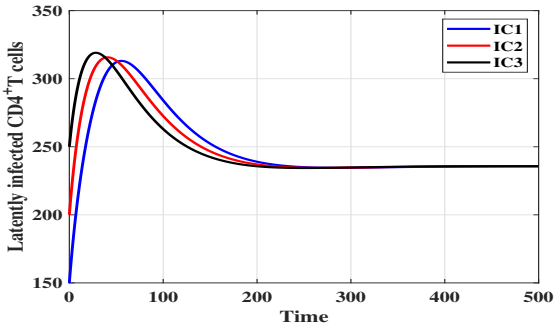

(f) Latently infected CD4$^+$T cells

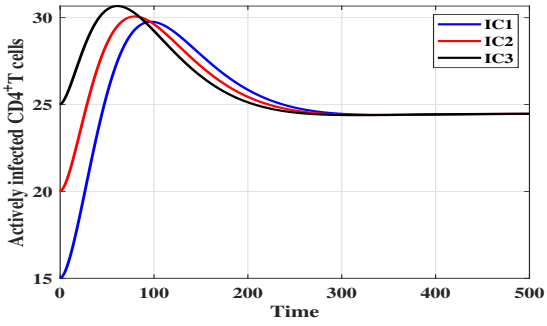

(g) Actively infected CD4$^+$T cells

Figure 3. Solutions of the system described by (2.1)–(2.7) with the initial conditions IC1–IC3 in Case 2.

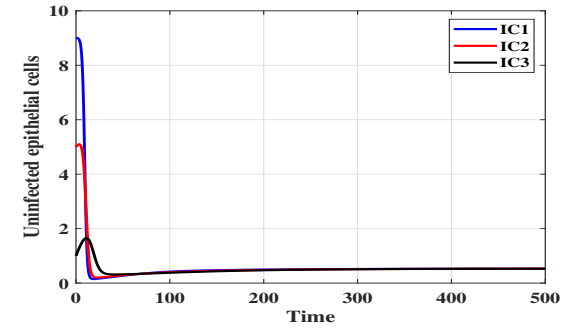

(a) Uninfected epithelial cells

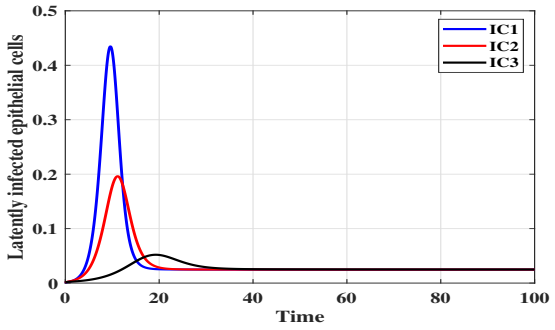

(b) Latently infected epithelial cells

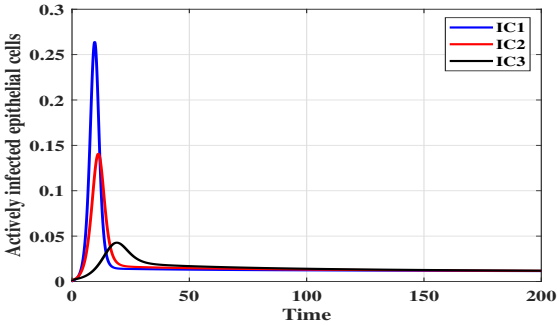

(c) Actively infected epithelial cells

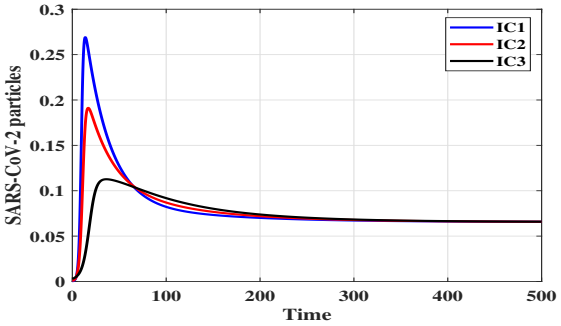

(d) SARS-CoV-2 particles

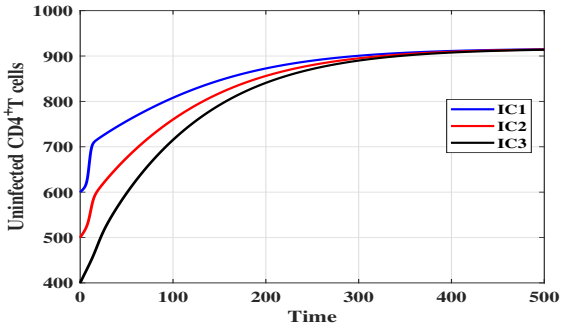

(e) Uninfected CD4$^+$T cells

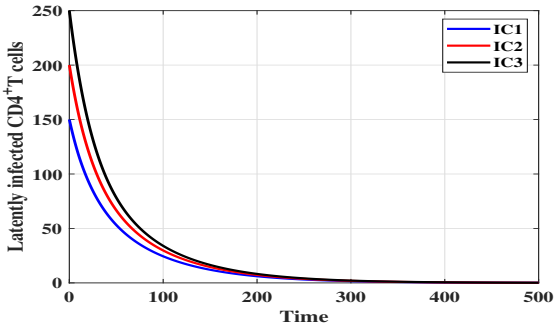

(f) Latently infected CD4$^+$T cells

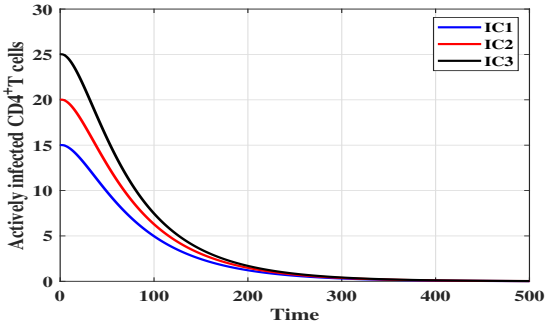

(g) Actively infected CD4$^+$T cells

Figure 4. Solutions of the system described by (2.1)–(2.7) with the initial conditions IC1–IC3 in Case 3.

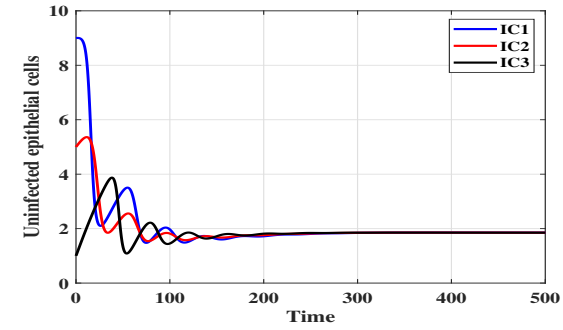

(a) Uninfected epithelial cells

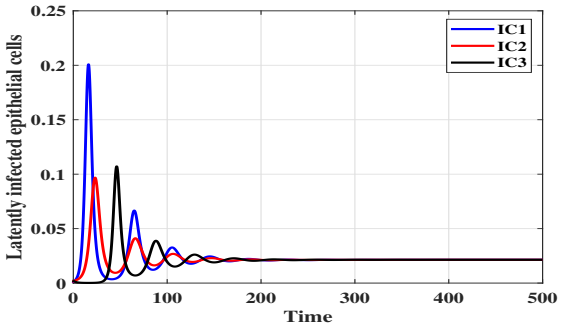

(b) Latently infected epithelial cells

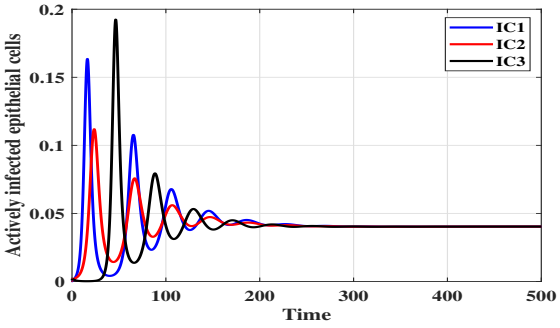

(c) Actively infected epithelial cells

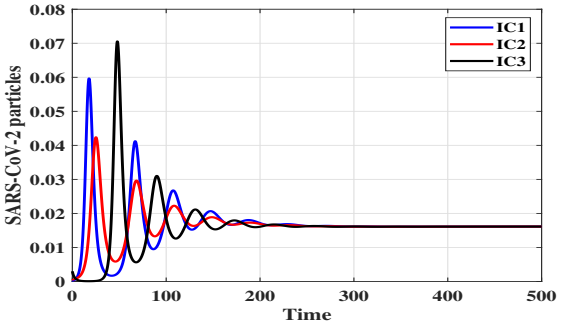

(d) SARS-CoV-2 particles

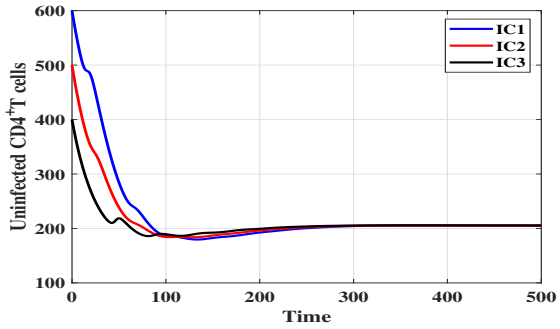

(e) Uninfected $CD4^+T$ cells

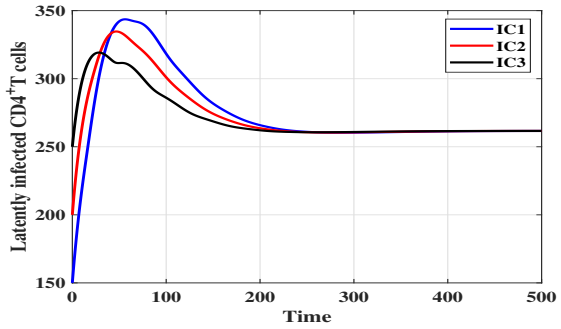

(f) Latently infected $CD4^+T$ cells

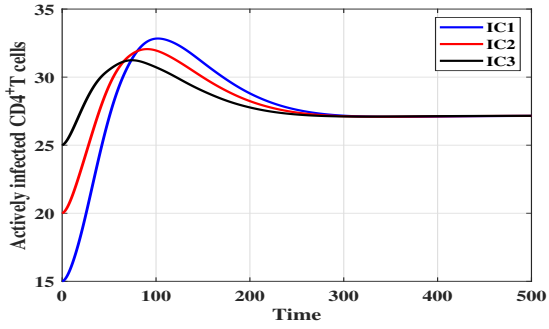

(g) Actively infected $CD4^+T$ cells

Figure 5. Solutions of the system described by (2.1)–(2.7) with the initial conditions IC1–IC3 in Case 4.

The Jacobian matrix $J = J(X, N, Y, V, U, L, A)$ can be calculated as follows:

$$J = \begin{pmatrix} -(\rho V + \xi_X) & 0 & 0 & -\rho X & 0 & 0 & 0 \\ \rho V & -(\kappa + \xi_N) & 0 & \rho X & 0 & 0 & 0 \\ 0 & \kappa & -(\mu U + \xi_Y) & 0 & -\mu Y & 0 & 0 \\ 0 & 0 & \eta & -\xi_V & 0 & 0 & 0 \\ 0 & 0 & \theta U & 0 & \theta Y - \pi A - \xi_U & 0 & -\pi U \\ 0 & 0 & 0 & 0 & \pi A & -(\alpha + \xi_L) & \pi U + \omega\varepsilon^* \\ 0 & 0 & 0 & 0 & 0 & \alpha & (1-\omega)\varepsilon^* - \xi_A^* \end{pmatrix}.$$

At each equilibrium point, we compute the eigenvalues λ_j, $j = 1, 2, ..., 7$ of J. If $\mathrm{Re}(\lambda_j) < 0$, $j = 1, 2, ..., 7$, then the equilibrium point is locally stable. We select the parameters ρ, μ, ξ_V and π as given in Cases 1–4; then, we compute all nonnegative equilibria and the accompanying eigenvalues. Table 3 outlines the nonnegative equilibria, the real parts of the eigenvalues and whether or not the equilibrium point is stable. We found that the local stability agrees with the global one.

Table 3. Local stability of nonnegative equilibria in Cases 1– 4.

Case	Equilibrium point	$\mathrm{Re}(\lambda_i), i = 1, 2, ..., 7$	Stability
Case 1	$EP_0 = (10, 0, 0, 0, 833.33, 0, 0)$	$(-916.77, -5.51, -4.18, -0.048, -0.014, -0.012, -0.011)$	stable
Case 2	$EP_0 = (10, 0, 0, 0, 833.33, 0, 0)$	$(-916.77, -5.50, -4.19, -0.092, -0.012, -0.011, +0.031)$	unstable
	$EP_1 = (10, 0, 0, 0, 205.33, 235.70, 24.47)$	$(-225.98, -5.52, -4.17, -0.077, -0.017, -0.017, -0.011)$	stable
Case 3	$EP_0 = (10, 0, 0, 0, 833.33, 0, 0)$	$(-6.65, -6.65, -0.048, -0.014, -0.012, -0.011, +0.631)$	unstable
	$EP_2 = (0.529, 0.025, 0.011, 0.066, 916.87, 0, 0)$	$(-9.24, -4.27, -0.154, -0.051, -0.049, -0.013, -0.012)$	stable
Case 4	$EP_0 = (10, 0, 0, 0, 833.33, 0, 0)$	$(-6.71, -6.71, -0.092, -0.012, -0.011, +0.031, +0.18)$	unstable
	$EP_1 = (10, 0, 0, 0, 205.33, 235.70, 24.47)$	$(-4.03, -4.03, -0.077, -0.017, -0.017, -0.011, +1.10)$	unstable
	$EP_2 = (7.42, 0.007, 0.003, 0.001, 856.07, 0, 0)$	$(-7.85, -5.61, -0.093, -0.012, -0.007, -0.007, +0.031)$	unstable
	$EP_3 = (1.85, 0.021, 0.04, 0.016, 205.33, 261.62, 27.16)$	$(-3.48, -3.48, -0.078, -0.025, -0.025, -0.017, -0.017)$	stable

6.2. Comparison results

In this subsection, we present a comparison between the HTLV-I single infection and the coinfection with HTLV-I and SARS-CoV-2. We compare the solutions of the model described by (2.1)–(2.7) and the following SARS-CoV-2 mono-infection model:

$$\begin{cases} \dot{X} = \delta - \xi_X X - \rho V X, \\ \dot{N} = \rho V X - (\kappa + \xi_N) N, \\ \dot{Y} = \kappa N - \xi_Y Y - \mu Y U, \\ \dot{V} = \eta Y - \xi_V V, \\ \dot{U} = \gamma + \theta Y U - \xi_U U. \end{cases}$$

We consider $\rho = 3$, $\mu = 0.01$, $\xi_V = 0.6$ and $\pi = 0.0015$ with the initial condition IC3. We observe from Figure 6 that the presence of HTLV-I reduces the concentrations of uninfected epithelial cells and uninfected $CD4^+$T cells, while it increases the concentrations of latently SARS-CoV-2-infected epithelial cells, actively SARS-CoV-2-infected epithelial cells and free SARS-CoV-2 particles. This means that HTLV-I suppresses the immune response and enhances the SARS-CoV-2 infection.

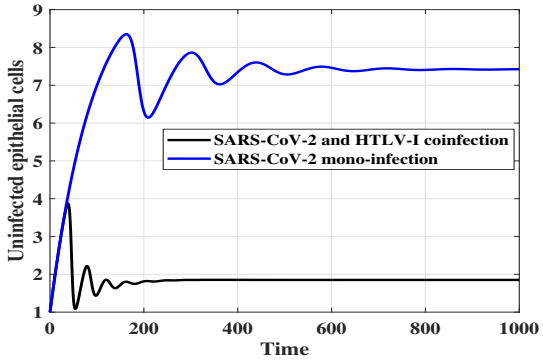

(a) Uninfected epithelial cells

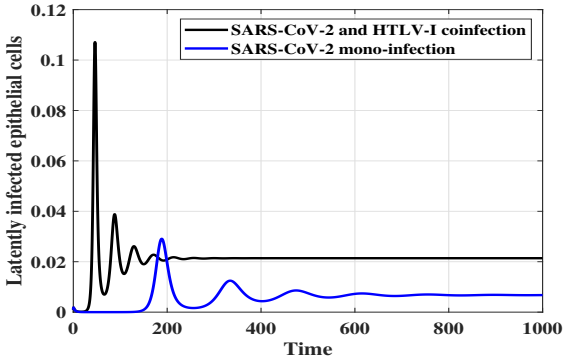

(b) Latently infected epithelial cells

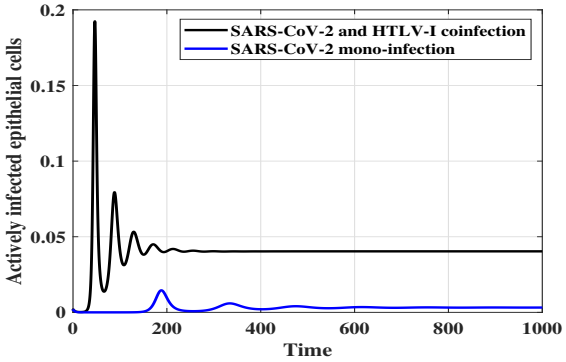

(c) Actively infected epithelial cells

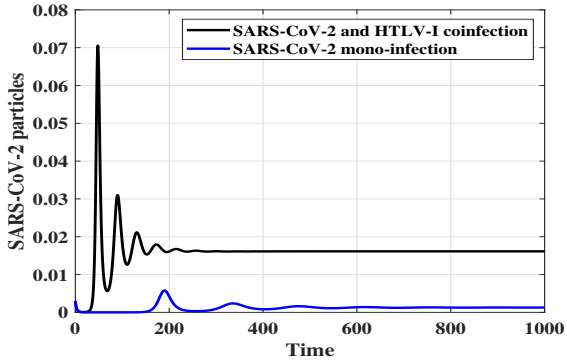

(d) SARS-CoV-2 particles

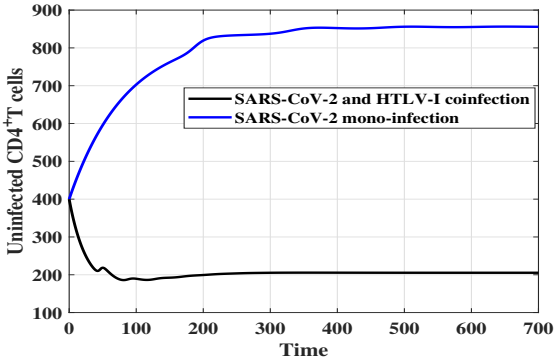

(e) Uninfected $CD4^{+}T$ cells

Figure 6. Comparison between the solutions of the SARS-CoV-2 mono-infection model and SARS-CoV-2/HTLV-I coinfection model.

7. Discussion

SARS-CoV-2 and HTLV-I coinfection cases were reported in [3] and [12]. Therefore, it is important to understand the within-host dynamics of this coinfection. In this paper, we developed and examined a within-host SARS-CoV-2 and HTLV-I coinfection model. We studied the basic and global properties of the model. We found that the system has four equilibria, and we proved the following:

(I) The uninfected equilibrium point EP_0 always exists. It is globally asymptotically stable when $R_1 \leq 1$ and $R_2 \leq 1$. This result suggests that, when $R_1 \leq 1$ and $R_2 \leq 1$, both SARS-CoV-2 and HTLV-I infections are predicted to die out regardless of the initial conditions. From a control viewpoint, setting $R_1 \leq 1$ and $R_2 \leq 1$ will be a good strategy. The parameter R_2 may be reduced by multiplying the parameters by ρ or η by $(1-\epsilon_1)$ or $(1-\epsilon_2)$, respectively. Here, $\epsilon_1 \in [0,1]$ and $\epsilon_2 \in [0,1]$ represent the effectiveness of antiviral drugs for blocking the infection and production of SARS-CoV-2 particles, respectively [18]. Since there is no treatment for HTLV-I infection, $R_1 \leq 1$ is rarely achieved.

(II) The HTLV-I mono-infection equilibrium point EP_1 exists if $R_1 > 1$. It is globally asymptotically stable when $R_1 > 1$ and $R_4 \leq 1$. This result establishes that, when $R_1 > 1$ and $R_4 \leq 1$, the HTLV-I mono-infection is always established, regardless of the initial conditions.

(III) The SARS-CoV-2 mono-infection equilibrium point EP_2 exists if $R_2 > 1$. It is globally asymptotically stable when $R_2 > 1$ and $R_3 \leq 1$. This result shows that, when $R_2 > 1$ and $R_3 \leq 1$, the SARS-CoV-2 mono-infection is always established, regardless of the initial conditions.

(IV) The HTLV-I and SARS-CoV-2 coinfection equilibrium point EP_3 exists if $R_3 > 1$ and $R_4 > 1$. It is globally asymptotically stable when $R_4 > 1$ and $1 < R_3 \leq 1 + \hat{R}$. This result shows that, when $R_4 > 1$ and $1 < R_3 \leq 1 + \hat{R}$, the HTLV-I and SARS-CoV-2 coinfection is always established, regardless of the initial conditions.

We discussed the impact of HTLV-I infection on the SARS-CoV-2 mono-infection dynamics. We found that the presence of HTLV-I suppresses the immune response and enhances the SARS-CoV-2 infection. This result agrees with [3], where it was reported that HTLV-I can cause immune dysfunction even in asymptomatic carriers. Therefore, HTLV-I may increase the risk of COVID-19.

The main limitation of the present research work is that we did not use real data to estimate the values of the model's parameters. The reasons are as follows: (i) The real measurements from HTLV-I/COVID-19 coinfection patients are still very limited; (ii) Comparing our results with a small number of real studies may not be very precise; (iii) Collecting real data from patients with HTLV-I and COVID-19 coinfection is not an easy task. Thus, the theoretical results obtained in the present paper need to be tested against empirical findings when real data become available.

8. Conclusions

Mathematical models are frequently used to understand the complex behavior of biological systems. In this paper, we constructed a new SARS-CoV-2/HTLV-I coinfection model within a host. The model considers the interactions between uninfected epithelial cells, latently SARS-CoV-2-infected epithelial cells, actively SARS-CoV-2-infected epithelial cells, free SARS-CoV-2 particles, uninfected $CD4^+T$ cells, latently HTLV-I-infected $CD4^+T$ cells and actively HTLV-I-infected $CD4^+T$ cells. We examined the nonnegativity and boundedness of the solutions. We calculated the equilibrium points of the model and established the conditions of their existence and stability. We established the global stability of

all equilibrium points by formulating suitable Lyapunov functions and applying LaSalle's invariance principle. We conducted some numerical simulations and showed that they are consistent with the analytical results. We discussed the effect of HTLV-I infection on the dynamics of SARS-CoV-2 mono-infection. We found that HTLV-I infection suppresses the immune response and enhances the SARS-CoV-2 infection; thus, it may increase the risk of COVID-19.

The model developed in this work can be improved by (i) utilizing real data to find a good estimation of the parameters' values, (ii) studying the effect of intracellular time delays [25], (iii) considering the mutations of SARS-CoV-2 [58, 66] and (iv) including the stochastic interaction. Memory is an important characteristic of viral infections. It will be interesting to examine the effect of memory on the dynamics of SARS-CoV-2 and HTLV-I coinfection via formulation of the model through the use of fractional differential equations [67]. These research points need further investigation, so we leave them to future works.

Acknowledgment

This project was funded by the Deanship of Scientific Research (DSR), King Abdulaziz University, Jeddah, Saudi Arabia, under grant no. (KEP-PhD-38-130-43). The authors, therefore, acknowledge, with thanks, the DSR for technical and financial support.

Conflict of interest

The authors declare that there is no conflict of interest.

References

1. World Health Organization (WHO), Coronavirus disease (COVID-19): weekly epidemiological update, 2022. Available from: https://pesquisa.bvsalud.org/portal/resource/pt/who-334188.
2. World Health Organization (WHO), COVID-19 vaccine tracker, 2020. Available from: https://covid19.trackvaccines.org/agency/who/.
3. T. Enomoto, T. Shiroyama, H. Hirata, S. Amiya, Y. Adachi, T. Niitsu, et al., COVID-19 in a human T-cell lymphotropic virus type-1 carrier, *Clin. Case Rep.*, **10** (2022), e05463. https://doi.org/10.1002/ccr3.5463
4. X. Zhu, Y. Ge, T. Wu, K. Zhao, Y. Chen, B. Wu, et al., Co-infection with respiratory pathogens among COVID-2019 cases, *Virus Res.*, **285** (2020), 198005. https://doi.org/10.1016/j.virusres.2020.198005
5. P. S. Aghbash, N. Eslami, M. Shirvaliloo, H. B. Baghi, Viral coinfections in COVID-19, *J. Med. Virol.*, **93** (2021), 5310–5322. https://doi.org/10.1002/jmv.27102
6. M. D. Nowak, E. M. Sordillo, M. R. Gitman, A. E. Paniz Mondolfi, Coinfection in SARS-CoV-2 infected patients: Where are influenza virus and rhinovirus/enterovirus? *J. Med. Virol.*, **92** (2020), 1699–1700. https://doi.org/10.1002/jmv.25953

7. E. A. Hernandez-Vargas, E. Wilk, L. Canini, F. R. Toapanta, S. C. Binder, A. Uvarovskii, et al., Effects of aging on influenza virus infection dynamics, *J. Virol.*, **88** (2014), 4123–4131. https://doi.org/10.1128/JVI.03644-13
8. R. V. Luckheeram, R. Zhou, A. D. Verma, B. Xia, $CD4^+$T Cells: Differentiation and functions, *J. Immunol. Res.*, **2012** (2012), 925135. https://doi.org/10.1155/2012/925135
9. D. Wodarz, C. R. M. Bangham, Evolutionary dynamics of HTLV-I, *J. Mol. Evol.*, **50** (2000), 448–455. https://doi.org/10.1007/s002390010047
10. World Health Organization (WHO), Human T-lymphotropic virus type 1, 2022. Available from: `https://who.int/news-room/fact-sheets/detail/human-t-lymphotropic-virus-type-1`
11. F. A. Proietti, A. B. F. Carneiro-Proietti, B. C. Catalan-Soares, E. L. Murphy, Global epidemiology of HTLV-I infection and associated diseases, *Oncogene*, **24** (2005), 6058–6068. https://doi.org/10.1038/sj.onc.1208968
12. R. Hosoba, S. Makita, M. Shiotsuka, O. Kobayashi, K. Nakano, M. Muroya, et al., COVID-19 pneumonia in a patient with adult T-cell leukemia-lymphoma, *J. Clin. Exp. Hematop.*, **60** (2020), 174–178. https://doi.org/10.3960/jslrt.20030
13. E. A. Hernandez Vargas, J. Velasco-Hernandez, In-host modelling of COVID-19 in humans, *Annu. Rev. Control*, **50** (2020), 448–456. https://doi.org/10.1016/j.arcontrol.2020.09.006
14. C. Li, J. Xu, J. Liu, Y. Zhou, The within-host viral kinetics of SARS-CoV-2, *Math. Biosci. Eng.*, **17** (2020), 2853–2861. https://doi.org/10.3934/mbe.2020159
15. R. Ke, C. Zitzmann, D. D. Ho, R. M. Ribeiro, A. S. Perelson, In vivo kinetics of SARS-CoV-2 infection and its relationship with a person's infectiousness, *Proc. Natl. Acad. Sci. USA*, **118** (2021), e2111477118. https://doi.org/10.1073/pnas.2111477118
16. A. Gonçalves, J. Bertrand, R. Ke, E. Comets, X. De Lamballerie, D. Malvy, et al., Timing of antiviral treatment initiation is critical to reduce SARS-CoV-2 viral load, *CPT Pharmacomet. Syst.*, **9** (2020), 509–514. https://doi.org/10.1002/psp4.12543
17. S. Wang, Y. Pan, Q. Wang, H. Miao, A. N. Brown, L. Rong, Modeling the viral dynamics of SARS-CoV-2 infection, *Math. Biosci.*, **328** (2020), 108438. https://doi.org/10.1016/j.mbs.2020.108438
18. I. Ghosh, Within host dynamics of SARS-CoV-2 in humans: Modeling immune responses and antiviral treatments, *SN Comput. Sci.*, **2** (2021), 482. https://doi.org/10.1007/s42979-021-00919-8
19. K. Hattaf, N. Yousfi, Dynamics of SARS-CoV-2 infection model with two modes of transmission and immune response, *Math. Biosci. Eng.*, **17** (2020), 5326–5340. https://doi.org/10.3934/mbe.2020288
20. A. E. S. Almocera, G. Quiroz, E. A. Hernandez-Vargas, Stability analysis in COVID-19 within-host model with immune response, *Commun. Nonlinear Sci.*, **95** (2021), 105584. https://doi.org/10.1016/j.cnsns.2020.105584
21. J. Mondal, P. Samui, A. N. Chatterjee, Dynamical demeanour of SARS-CoV-2 virus undergoing immune response mechanism in COVID-19 pandemic, *Eur. Phys. J. Spec. Top.*, **231** (2022), 3357–3370. https://doi.org/10.1140/epjs/s11734-022-00437-5
22. S. Chowdhury, J. Chowdhury, S. Ahmed, P. Agarwal, I. Badruddin, S. Kamangar, Mathematical modelling of COVID-19 disease dynamics: Interaction between immune system and SARS-CoV-2 within host, *AIMS Math.*, **7** (2022), 2618–2633. https://doi.org/10.3934/math.2022147

23. P. Abuin, A. Anderson, A. Ferramosca, E. A. Hernandez-Vargas, A. H. Gonzalez, Characterization of SARS-CoV-2 dynamics in the host, *Annu. Rev. Control*, **50** (2020), 457–468. https://doi.org/10.1016/j.arcontrol.2020.09.008
24. B. Chhetri, V. M. Bhagat, D. K. K. Vamsi, V. S. Ananth, D. B. Prakash, R. Mandale, et al., Within-host mathematical modeling on crucial inflammatory mediators and drug interventions in COVID-19 identifies combination therapy to be most effective and optimal, *Alex. Eng. J.*, **60** (2021), 2491–2512. https://doi.org/10.1016/j.aej.2020.12.011
25. A. M. Elaiw, A. J. Alsaedi, A. D. Al Agha, A. D. Hobiny, Global stability of a humoral immunity COVID-19 model with logistic growth and delays, *Mathematics*, **10** (2022), 1857. https://doi.org/10.3390/math10111857
26. A. ul Rehman, R. Singh, P. Agarwal, Modeling, analysis and prediction of new variants of covid-19 and dengue co-infection on complex network, *Chaos Soliton. Fract.*, **150** (2021), 111008. https://doi.org/10.1016/j.chaos.2021.111008
27. M. M. Ojo, T. O. Benson, O. J. Peter, E. F. D. Goufo, Nonlinear optimal control strategies for a mathematical model of COVID-19 and influenza co-infection, *Physica A*, **607** (2022), 128173. https://doi.org/10.1016/j.physa.2022.128173
28. N. Ringa, M. L. Diagne, H. Rwezaura, A. Omame, S. Y. Tchoumi, J. M. Tchuenche, HIV and COVID-19 co-infection: A mathematical model and optimal control, *Informatics in Medicine Unlocked*, **31** (2022), 100978. https://doi.org/10.1016/j.imu.2022.100978
29. A. Omame, M. Abbas, C. P. Onyenegecha, Backward bifurcation and optimal control in a co-infection model for SARS-CoV-2 and ZIKV, *Results Phys.*, **37** (2022), 105481. https://doi.org/10.1016/j.rinp.2022.105481
30. A. Omame, M. Abbas, A. Abdel-Aty, Assessing the impact of SARS-CoV-2 infection on the dynamics of dengue and HIV via fractional derivatives, *Chaos Soliton. Fract.*, **162** (2022), 112427. https://doi.org/10.1016/j.chaos.2022.112427
31. K. G. Mekonen, L. L. Obsu, Mathematical modeling and analysis for the co-infection of COVID-19 and tuberculosis, *Heliyon*, **8** (2022), e11195. https://doi.org/10.1016/j.heliyon.2022.e11195
32. A. G. C. Pérez, D. A. Oluyori, A model for COVID-19 and bacterial pneumonia coinfection with community- and hospital-acquired infections, *Math. Model. Numer. Simul. Appl.*, **2** (2022), 197–210. https://doi.org/10.53391/mmnsa.2022.016
33. A. M. Elaiw, A. D. Al Agha, Global dynamics of SARS-CoV-2/cancer model with immune responses, *Appl. Math. Comput.*, **408** (2021), 126364. https://doi.org/10.1016/j.amc.2021.126364
34. Y. Zhou, M. Huang, Y. Jiang, X. Zou, Data-driven mathematical modeling and dynamical analysis for SARS-CoV-2 coinfection with bacteria, *Int. J. Bifurcat. Chaos*, **31** (2021), 2150163. https://doi.org/10.1142/S0218127421501637
35. A. M. Elaiw, A. D. Al Agha, S. A. Azoz, E. Ramadan, Global analysis of within-host SARS-CoV-2/HIV coinfection model with latency, *Eur. Phys. J. Plus*, **137** (2022), 174. https://doi.org/10.1140/epjp/s13360-022-02387-2
36. A. D. Al Agha, A. M. Elaiw, S. A. Azoz, E. Ramadan, Stability analysis of within-host SARS-CoV-2/HIV coinfection model, *Math. Method. Appl. Sci.*, **45** (2022), 11403–11422. https://doi.org/10.1002/mma.8457

37. A. D. Al Agha, A. M. Elaiw, Global dynamics of SARS-CoV-2/malaria model with antibody immune response, *Math. Biosci. Eng.*, **19** (2022), 8380–8410. https://doi.org/10.3934/mbe.2022390
38. A. M. Elaiw, A. D. Al Agha, Global stability of a reaction-diffusion Malaria/COVID-19 coinfection dynamics model, *Mathematics*, **10** (2022), 4390. https://doi.org/10.3390/math10224390
39. A. M. Elaiw, R. S. Alsulami, A. D. Hobiny, Modeling and stability analysis of within-host IAV/SARS-CoV-2 coinfection with antibody immunity, *Mathematics*, **10** (2022), 4382. https://doi.org/10.3390/math10224382
40. L. Pinky, H. M. Dobrovolny, SARS-CoV-2 coinfections: Could influenza and the common cold be beneficial? *J. Med. Virol.*, **92** (2020), 2623–2630. https://doi.org/10.1002/jmv.26098
41. B. J. Nath, K. Dehingia, V. N. Mishra, Y. Chu, H. K. Sarmah, Mathematical analysis of a within-host model of SARS-CoV-2, *Adv. Differ. Equ.*, **2021** (2021), 113. https://doi.org/10.1186/s13662-021-03276-1
42. N. I. Stilianakis, J. Seydel, Modeling the T-cell dynamics and pathogenesis of HTLV-I infection, *Bull. Math. Biol.*, **61** (1999), 935–947. https://doi.org/10.1006/bulm.1999.0117
43. X. Pan, Y. Chen, H. Shu, Rich dynamics in a delayed HTLV-I infection model: Stability switch, multiple stable cycles, and torus, *J. Math. Anal. Appl.*, **479** (2019), 2214–2235. https://doi.org/10.1016/j.jmaa.2019.07.051
44. H. Gomez-Acevedo, M. Y. Li, S. Jacobson, Multistability in a model for CTL response to HTLV-I infection and its implications to HAM/TSP development and prevention, *Bull. Math. Biol.*, **72** (2010), 681–696. https://doi.org/10.1007/s11538-009-9465-z
45. Y. Wang, J. Liu, J. M. Heffernan, Viral dynamics of an HTLV-I infection model with intracellular delay and CTL immune response delay, *J. Math. Anal. Appl.*, **459** (2018), 506–527. https://doi.org/10.1016/j.jmaa.2017.10.027
46. F. Li, W. Ma, Dynamics analysis of an HTLV-1 infection model with mitotic division of actively infected cells and delayed CTL immune response, *Math. Method. Appl. Sci.*, **41** (2018), 3000–3017. https://doi.org/10.1002/mma.4797
47. S. Li, Y. Zhou, Backward bifurcation of an HTLV-I model with immune response, *Discrete Cont. Dyn. B*, **21** (2016), 863–881. https://doi.org/10.3934/dcdsb.2016.21.863
48. M. Y. Li, A. G. Lim, Modelling the role of Tax expression in HTLV-IPersistence in vivo, *Bull. Math. Biol.*, **73** (2011), 3008–3029. https://doi.org/10.1007/s11538-011-9657-1
49. A. G. Lim, P. K. Maini, HTLV-I infection: A dynamic struggle between viral persistence and host immunity, *J. Theor. Biol.*, **352** (2014), 92–108. https://doi.org/10.1016/j.jtbi.2014.02.022
50. S. Khajanchi, S. Bera, T. K. Roy, Mathematical analysis of the global dynamics of a HTLV-I infection model, considering the role of cytotoxic T-lymphocytes, *Math. Comput. Simulat.*, **180** (2021), 354–378. https://doi.org/10.1016/j.matcom.2020.09.009
51. P. Katri, S. Ruan, Dynamics of human T-cell lymphotropic virus I (HTLV-I) infection of $CD4^+$T-cells, *C. R. Biol.*, **327** (2004), 1009–1016. https://doi.org/10.1016/j.crvi.2004.05.011
52. Y. Wang, J. Liu, Global stability for delay-dependent HTLV-I model with CTL immune response, In: *AIP Conference Proceedings*, **1738** (2016), 480074. https://doi.org/10.1063/1.4952310

53. S. Bera, S. Khajanchi, T. K. Roy, Dynamics of an HTLV-I infection model with delayed CTLs immune response, *Appl. Math. Comput.*, **430** (2022), 127206. https://doi.org/10.1016/j.amc.2022.127206

54. W. Wang, W. Ma, Global dynamics of a reaction and diffusion model for an HTLV-I infection with mitotic division of actively infected cells, *J. Appl. Anal. Comput.*, **7** (2017), 899–930. https://doi.org/10.11948/2017057

55. A. M. Elaiw, A. S. Shflot, A. D. Hobiny, Stability analysis of general delayed HTLV-I dynamics model with mitosis and CTL immunity, *Math. Biosci. Eng.*, **19** (2022), 12693–12729. https://doi.org/10.3934/mbe.2022593

56. A. M. Elaiw, N. H. AlShamrani, Analysis of a within-host HIV/HTLV-I co-infection model with immunity, *Virus Res.*, **295** (2021), 198204. https://doi.org/10.1016/j.virusres.2020.198204

57. A. M. Elaiw, N. H. AlShamrani, HTLV/HIV dual infection: Modeling and analysis, *Mathematics*, **9** (2021), 51. https://doi.org/10.3390/math9010051

58. N. Bellomo, D. Burini, N. Outada, Multiscale models of Covid-19 with mutations and variants, *Netw. Heterog. Media*, **17** (2022), 293–310. https://doi.org/10.3934/nhm.2022008

59. H. L. Smith, P. Waltman, *The theory of the chemostat: Dynamics of microbial competition*, Cambridge University Press, 1995.

60. A. Korobeinikov, Global properties of basic virus dynamics models, *Bull. Math. Biol.*, **66** (2004), 879–883. https://doi.org/10.1016/j.bulm.2004.02.001

61. A. Korobeinikov, Global properties of infectious disease models with nonlinear incidence, *Bull. Math. Biol.*, **69** (2007), 1871–1886. https://doi.org/10.1007/s11538-007-9196-y

62. H. K. Khalil, *Nonlinear systems*, Prentice Hall, 2002.

63. A. S. Perelson, D. E. Kirschner, R. De Boer, Dynamics of HIV infection of $CD4^+$T cells, *Math. Biosci.*, **114** (1993), 81–125. https://doi.org/10.1016/0025-5564(93)90043-A

64. M. Prakash, R. Rakkiyappan, A. Manivannan, J. Cao, Dynamical analysis of antigen-driven T-cell infection model with multiple delays, *Appl. Math. Comput.*, **354** (2019), 266–281. https://doi.org/10.1016/j.amc.2019.02.050

65. B. Asquith, C. R. M. Bangham, Quantifying HTLV-I dynamics, *Immunol. Cell Biol.*, **85** (2007), 280–286. https://doi.org/10.1038/sj.icb.7100050

66. N. Bellomo, D. Burini, N. Outada, Pandemics of mutating virus and society: a multi-scale active particles approach, *Philos. Trans. A. Math. Phys. Eng. Sci.*, **380** (2022), 20210161. https://doi.org/10.1098/rsta.2021.0161

67. A. N. Chatterjee, F. Al Basir, M. A. Almuqrin, J. Mondal, I. Khan, SARS-CoV-2 infection with lytic and nonlytic immune responses: A fractional order optimal control theoretical study, *Results Phys.*, **26** (2021), 104260. https://doi.org/10.1016/j.rinp.2021.104260

AIMS Press